RSC Advances

PAPER

View Article Online
View Journal | View Issue

Cite this: *RSC Adv.*, 2022, **12**, 15196

Effects of active compounds from *Cassia fistula* on quorum sensing mediated virulence and biofilm formation in *Pseudomonas aeruginosa*†

Zoya Peerzada,[a] Ashish M. Kanhed[b] and Krutika B. Desai *[c]

Pseudomonas aeruginosa infections are attributed to its ability to form biofilms and are difficult to eliminate with antibiotic treatment. Biofilm formation is regulated by quorum sensing (QS), an intracellular bacterial communication mechanism that allows the activation of numerous virulence factors and secondary metabolites. Targeting the QS pathway is a potential approach that prevents QS-controlled phenotypes and biofilm formation. For the first time, the current work has identified antiquorum sensing activity in the partially purified four fractions from the hot ethyl acetate extract of *Cassia fistula* fruit pods. Of the four fractions, only fraction-1 gave decreased AHL activity; the phytoconstituents in this fraction were identified as rhein, 3-aminodibenzofuran, 5-(hydroxymethyl)-2-(dimethoxymethyl)furan, and dihydrorhodamine. Fraction-1 (1 mg ml^{-1}) and rhein (0.15 mg ml^{-1}) showed 63% and 42.7% reduction in short-chain AHL production, respectively, without hindering the bacterial growth. Fraction-1 inhibited QS-mediated extracellular virulence factors *viz.* protease, elastase, pyocyanin, and rhamnolipid ($p < 0.05$). Quantitative analysis of biofilm formation showed 77% & 62.4% reduction by fraction-1 (1 mg ml^{-1}) and rhein (0.15 mg ml^{-1}) respectively. Confocal laser microscopy (CLMS) & scanning electron microscopy (SEM) confirmed the reduction of biofilm formation in *Pseudomonas aeruginosa* upon treatment with fraction-1 and rhein. Moreover, the *in vivo* study displayed that fraction-1 and rhein (standard) significantly enhanced the survival of *Caenorhabditis elegans* by suppressing the potency of virulence factors of *Pseudomonas aeruginosa*. Quantitative real-time polymerase chain reaction results demonstrated the down-regulation of QS-related genes, lasI, lasR, rhlI, and rhlR. In addition, *in silico* analysis divulged that a component identified by GC-MS displayed a strong affinity towards *Las*I and *Las*R. These findings suggest that potent phytochemicals from fraction-1, including rhein, could serve as novel phytotherapeutics in controlling emerging infections of antibiotic-resistant bacterial pathogens like *Pseudomonas aeruginosa*.

Received 14th November 2021
Accepted 5th April 2022

DOI: 10.1039/d1ra08351a

rsc.li/rsc-advances

1. Introduction

The pervasive use of antibiotics to treat bacterial infections has led to the emergence of drug resistance in microorganisms, resulting in a significant challenge for the healthcare sector in controlling bacterial infections.[1,2] Various mechanisms of antibiotic resistance include efflux pump mediated antibiotic elimination, chemical modification of antibiotics, and modification in drug target genes. Biofilms formation by many of the bacterial pathogens also poses a greater challenge in treatment than that of their planktonic counterparts. Poor penetration of antibiotics in biofilms matrix may manifest in antibiotic resistance in such pathogens. Consequently, there is a greater need for futuristic antibacterial molecules to treat various bacterial infections; however, inadequate new drug development poses a great challenge, especially for the healthcare sector in developing countries.[3,4]

Biofilm formation and extracellular virulence phenotypes are globally regulated by the well-defined cell-to-cell communication systems called quorum sensing (QS).[5,6] This system aids in synchronizing specific genes and determining bacterial pathogenesis. In Gram-negative bacteria, QS is controlled by diffusible auto-inducers molecules (*N*-acyl-L-homoserine lactones (AHL)).[7–9] *Pseudomonas aeruginosa* (*P. aeruginosa*), recognized as a malevolent pathogen, is a prime cause of numerous outbreaks of nosocomial infections. It is associated with a significant risk of drug resistance and facilitates biofilm establishment by successfully infecting many hosts.[10]

[a]*Sunandan Divatia School of Science, SVKM'S NMIMS (Deemed to be University), Mumbai-400056, India*

[b]*Shobhaben Pratapbhai Patel School of Pharmacy & Technology Management, SVKM's NMIMS University, Mumbai-400056, India*

[c]*SVKM's Mithibai College of Arts, Chauhan Institute of Science, Amrutben Jivanlal College of Commerce and Economics, Mumbai, 400056, India. E-mail: Krutika.Desai@mithibai.ac.in; Tel: +91 97690 80289*

† Electronic supplementary information (ESI) available. See https://doi.org/10.1039/d1ra08351a

In *P. aeruginosa*, virulence factor production is modulated by three hierarchical QS circuits – *Las*I/R, *Rhl*I/R, and *PQS* – that initiate the QS process using small autoinducer molecules *viz.* long acyl chain-HSL, 3-oxo-C12-HSL, as well as a short acyl chain-HSL, C4-HSL. These molecules collectively regulate the autoinduction loop for upregulation of several virulence factors and secondary metabolites (LasA, LasB, rhamnolipids, hydrogen cyanide, and pyocyanin) and tissue degrading enzymes (exoenzymes and exotoxins) in host cells. These virulence factors help bacteria to invade host tissues and initiate damage.[11] QS-mediated swimming, swarming & twitching motilities are vital factors in the spread and development of biofilms. Considering the involvement of QS in regulating numerous pathogenicity-associated genes, targeting and attenuating QS serves as a reliable target for the control of biofilm-forming MDR strains.[12]

The first anti-QS activity was reported in halogenated furanone isolated from marine red algae *Delisea pulchra*; however, this could not gain much popularity because of its toxic nature and instability.[13]

In the past few years, plant-based drug discovery has been gaining currency among researchers for exploring new modalities of drugs.[14] Natural-originated compounds are always considered in medical fields because they are biodegradable and usually very useful, and serve as a convenient compound for inhibiting biological infection.[15] Diterpene phytol was found to inhibit pyocyanin secretion, twitching motility, and biofilm production in *P. aeruginosa*.[16] A flavonoid, mosloflavone, was investigated against *P. aeruginosa* virulence and biofilm formation. It inhibited the pyocyanin production, LasB elastase, and QS regulated biofilm formation and development and exhibited promising potential in controlling bacterial infection in the *Caenorhabditis elegans* model system *in vivo*.[17] Various plant-derived QS inhibitors *viz.* coumarin, baicalein, curcumin, berberine, phillyrin, cinnamic acid, clove oil, zingerone, and quercetin have been surveyed and proven to be attractive anti-infective drug targets in pathogenic bacteria. Researchers have explored medicinal plants and their active components, but anti-QS hit molecules are still at an initial stage of development and need to be studied extensively.[18–27]

Cassia fistula is well known for its laxative properties due to anthraquinone compounds (rhein, aloe-emodin) in the pods. The anti-microbial activity of rhein (7.8–31.25 μg ml^{-1}) against "methicillin-resistant *Staphylococcus aureus* (MRSA) and methicillin-sensitive *Staphylococcus aureus* (MSSA)" strains have already been explored.[28] Azelmat *et al.* reported rhein for its potential to impair bacterial pathogenicity by reducing the transcriptional gene expression of periodontopathogenic bacterium *P. gingivalis*.[29] In a report by Ding *et al.*, 46 traditional Chinese medicines, including various anthraquinones, were screened for anti-QS activity through molecular docking against *P. aeruginosa* and *Stenotrophomonas maltophilia*.[30] Interestingly, study results showed that emodin conjointly with ampicillin showed the highest inhibition against *P. aeruginosa* rather than either of them alone.

To study the effect of *Cassia fistula* on the bacterial QS system, different fractions of the hot ethyl acetate extracts of fruit pods were obtained using flash chromatography-mass spectrometry. Fraction-1 was observed to be most effective against the QS network of *P. aeruginosa*. One of the active phytoconstituents of F-1, anthraquinone (rhein shown in Fig. 1), shares structural similarities with emodin, a known antivirulent molecule against certain bacterial pathogens.[30] Hence, the present work hypothesized to investigate the potential of isolated rhein-rich fraction (F-1) and pure rhein as an effective agent to fight against the QS circuitry of *P. aeruginosa*. Molecular docking was carried out to identify these phytoconstituents as putative QSIs.

2. Material and methods

2.1 Media and chemicals

All media *viz.* Brain Heart Infusion (BHI) agar, Luria–Bertani (LB) agar, and LB broth were procured from Hi-Media Laboratories, Mumbai. Propidium iodide (PI), rhamnose standard, Elastin Congo Red (ECR) & rhein were procured from Sigma-Aldrich (AMI Chemicals, Mumbai with ≥98% purity). Nucleic acid stain SYTO 9 green-fluorescent was obtained from Invitrogen™. All other organic solvents and chemicals were obtained from Qualigens Fine Chemicals, India, and flash-chromatography disposable columns (12 grams) from RediSep® Rf from Teledyne Isco US.

2.2 Bacterial strain and culture conditions

This study used *P. aeruginosa* PAO1 (ATCC15692) as a test strain; *Escherichia coli* MG4/PKDT17 (lasB:lacZ place-lasR Apr) and *C. violaceum* (ATCC12472) were used as reporter strains to evaluate the long-chain & short-chain AHLs, respectively. *Staphylococcus aureus* (MTCC737) strain was utilized for virulence factor protease. Sterile LB broth was used to revive all the bacterial cultures before conducting the experiments. Temperature conditions were maintained between 32 °C and 37 °C for all bacterial strains. *Caenorhabditis elegans* worms (wild-type strain) and *Escherichia coli* OP50 were received from the Tata Institute of Fundamental Research (TIFR), Mumbai, India. *E. coli* OP50 was propagated in the LB broth (37 °C). Nematode growth medium (NGM) agar plates, prior seeded with *E. coli* OP50, were used to grow nematodes (maintained at 21 °C) as a food source.

2.3 Collection of fruit pods, extraction, and purification of active components by flash chromatography

Cassia fistula (Aragvadha) fruit pods were collected from a local vendor in Mumbai in January 2017. Plant authentication was

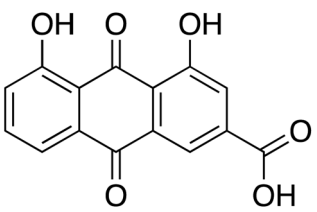

Fig. 1 Chemical structure of rhein ($C_{15}H_8O_6$), mol wt = 284.22 g mol^{-1}.

done from Blatter Herbarium, St. Xavier's College, Mumbai, India. The specimen is identical to the Blatter Herbarium specimen PD 5430 of P. Divakar. The fruit pods, pulp, and seeds were dried in the oven at 40 °C, powdered, and stored in an airtight container. 50 g of the material was extracted (Soxhlet) using ethyl acetate solvent (300 ml) at 30–45 °C. Eventually, extracts were filtered & dried using a rotary evaporator. The dried crude extract was subjected to successive purification using flash column chromatography (Teledyne ISCO), as described by Uckoo *et al.* previously, with modifications.[31] A RediSep® Rf column of 12 g packed with fine spherical silica gel (20–40 μm) and column volume capacity of 30 ml min^{-1} was used to purify the crude mixture's active component. 3 g of silica gel (60–120 mesh) impregnated crude ethyl acetate extract of *Cassia fistula* was loaded into the solid load cartridges. Before separation, the column was equilibrated and saturated with mobile phase ethyl acetate and hexane. The crude extract was separated using solvent A (hexane) and solvent B (ethyl acetate) gradient. Initially, 10% of solvent B was held for 4–5 min; later, it was linearly increased to 50% over 18–22 min, then 60% B over 6.5 min (21–26 min), slowly increased from 60% to 100% (26–34 min) and 100% B over 10 min. Overall run time was 40–42 min, with the flow rate maintained at 10 ml min^{-1}. A total of 70 fractions was eluted by continuous monitoring of the analytes at 254 nm and 280 nm wavelengths (chromatogram exhibited in ESI Fig. 1†). These fractions were pooled based on the TLC profile (Fig. 2A) and subsequently analyzed for anti-QS activity.

2.4 Fraction-based anti-quorum sensing (anti-QS) activity

2.4.1 Chromatography fractions were analyzed for their inhibition of short-chain AHL production. Inhibition of short-chain AHL production was analyzed using reporter strain *C. violaceum* 12472, which produces a short acyl-HSL (C6-HSL) that regulates the production of dark purple pigment, violacein.[32] Agar well diffusion assay was performed to evaluate inhibition of short acyl-HSLs. About 100 μl of all 4 fractions at concentrations (0.4 mg ml^{-1}, 0.6 mg ml^{-1}, 0.8 mg ml^{-1} and 1.0 mg ml^{-1}) and rhein (0.025 mg ml^{-1}, 0.05 mg ml^{-1}, 0.1 mg ml^{-1} and 0.15 mg ml^{-1}) were used for the assay. DMSO (0.08%) and azithromycin dihydrate (AZM) (4 μg ml^{-1}) were used as negative and positive controls, respectively. Inhibition was detected in terms of loss of pigment around the wells treated with the test fractions but with visible growth of bacteria.[33] F-1 and its main component rhein were selected for subsequent analysis.

2.5 Analysis of phytochemical of F-1

2.5.1 GC-mass spectrum analysis (GC-MS). GC-MS analysis was carried out at the Indian Institute of Technology, Bombay, India, with an Agilent 7890 instrument furnished with an FID detector and Head Space injector, Combipal autosampler, MS: Jeol, ionization: electron ionization, time of flight mass analyser, software: data analysis, library: Nist 2008, column utilized: HP 5 ms, dimensions: 30 mm × 0.25 mm ID × 0.25 μm film thickness, initial temperature 21–50 °C, 2 min hold time, room temperature, helium applied as a carrier gas, flow rate (1 ml min^{-1}). One μl volume was used for the final injection. Unknown compounds in the samples were identified by comparing the known spectrum of the compounds in the library (NIST 2008).[34]

2.5.2 Identification and quantification of rhein using LC-MS. Structural characterization of rhein was carried out on LC-MS (LC-MS-8040 Shimadzu Japan) instrument. The mass spectrometric data were analyzed using lab solution software. Kromasil-C18 column (diameter 4.6 × 100 mm) was employed to perform the chromatographic separation. The analysis was carried out in positive electron ionization mode. 10 μl of samples (rhein and F-1–1000 ppm of stock concentration) were injected into the instrument. Ultra-high pure nitrogen gas was used as collision gas. The flow rate of the mobile phase was maintained at 0.8 ml min^{-1}. 0.1% formic acid (30%) and acetonitrile (ACN) (70%) was used as a solvent system in an isocratic manner. The

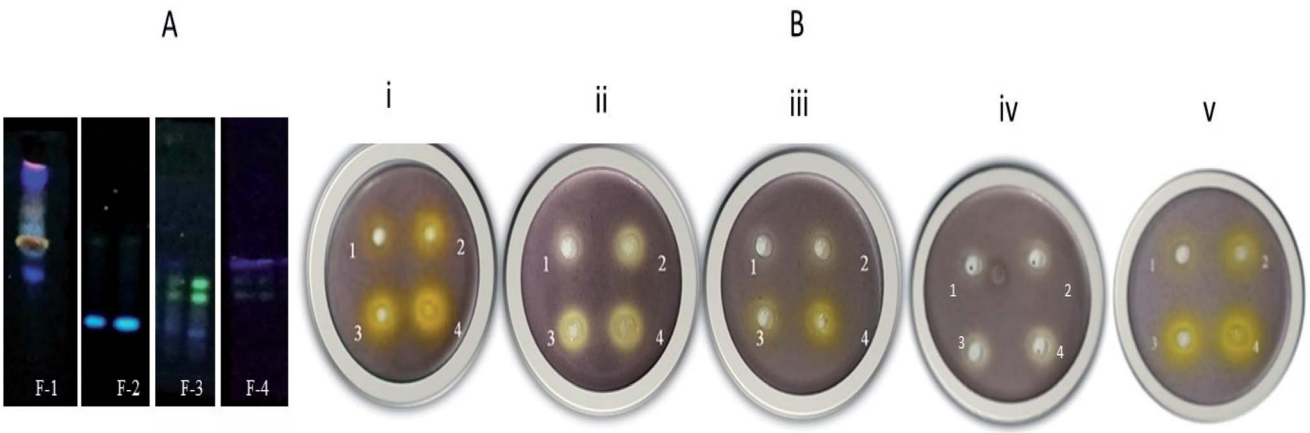

Fig. 2 (A) Thin layer chromatography (TLC) images of F-1 to F-4 extracted from flash chromatography (at 366 nm). (B) Inhibition of short-chain AHL in *C. violaceum* 12472 with increasing concentrations of various fractions *viz.* F-1, F-2, F-3, F-4 and main constituent of F-1, rhein. Plates (i), (ii), (iii), and (iv) represent 4 wells (well 1–0.4 mg ml^{-1}, well 2–0.6 mg ml^{-1}, well 3–0.8 mg ml^{-1}, well 4–1.0 mg ml^{-1}). Plate (v) represents rhein with varying concentrations (well 1–0.025 mg ml^{-1}, well 2–0.05 mg ml^{-1}, well 3–0.1 mg ml^{-1}, well 4–0.15 mg ml^{-1}).

total chromatographic run time was 5 minutes & column temperature was maintained at 27 °C[35] (ESI Fig. 3†).

2.6 Bacterial growth curve analysis

The effect of F-1 (0.6 mg ml^{-1}, 0.8 mg ml^{-1}, and 1 mg ml^{-1}) and rhein (0.15 mg ml^{-1}) on bacterial growth was analyzed by employing the method of Abraham *et al.* and Gala *et al.*[36,37] Various concentrations of F-1 and rhein were added to *P. aeruginosa* containing LB broth up to the final volume of 200 μl in 96 well plate. The alteration in cell density was measured at 600 nm every half-hour interval (Epoch 2 BioTek microplate reader). The growth curve was plotted by calculating the mean reduction in OD of 3 triplicates values ($n = 9$).

2.7 Quantitative analysis of violacein pigment production

Based on the screening results, the effect of F-1 and rhein on violacein production was quantified spectrophotometrically using a biomarker strain.[38] Briefly, overnight grown, *C. violaceum* 12472 was revived in fresh LB broth ($OD_{600} = 0.2$). To the above culture, samples (0.6–1 mg ml^{-1} of F-1 and 0.15 mg ml^{-1} for rhein) were supplemented and incubated overnight (the temperature at 31 °C) with continuous shaking (180 rpm). The next day, violacein pigments were pelleted by centrifuging the cultures (10 min at 12 880*g*). The collected cell pellet was disintegrated by employing pure DMSO, and further spectrophotometrically (PerkinElmer Lambda 25) was analyzed at 585 nm.[39] Finally, the percentage reduction in violacein pigment post-treatments with F-1 and rhein was calculated. Violacein was quantified using a molar extinction coefficient of 0.05601 ml μg^{-1} cm^{-1}.[40]

2.8 Effect of F-1 & rhein on long chain 3-oxo-C12-AHL

The levels of long-chain AHLs in F-1 and rhein treated bacterial culture supernatants were measured as per the procedure reported earlier.[37] AZM was used for comparing the results of the test sample. Briefly, overnight grown bacteria (OD_{600} = of 0.2) were mixed with F-1 and rhein and the controls (AZM and DMSO). These treated cultures were incubated at 32 °C overnight. The next day, the above cultures were centrifuged to obtain supernatant. Further, AHL containing supernatant was extracted using ethyl acetate (4–6 ml), and the solvent was evaporated by employing a nitrogen evaporator. The dried AHL in the tubes was reconstituted with 100 μl of sterile LB broth and further mixed with an *E. coli* MG4/PKDT17 culture ($OD_{600} = 0.4$). This reaction mixture was then incubated for 4–5 h and eventually pelleted. The pellet was solubilized in Z-buffer and mixed with 100 μl of chloroform, followed by 0.2% SDS. Finally, *O*-nitrophenyl-β-galactoside (ONPG) was added to the above solution, and the Miller assay (Miller 1972) was employed to measure β-galactosidase activity. Three independent assays in triplicate were performed ($n = 9$).[41]

2.9 Estimation of the extracellular virulence factors

2.9.1 Supernatant preparation. Overnight grown *P. aeruginosa* was inoculated in the appropriate medium and grown till OD reached 0.2 at 600 nm, and this culture was used for all the assays. AZM was prepared by dissolving in phosphate buffer saline and ethanol [PBS : EtOH (1 : 1)]. Kings' B medium was used for pyocyanin estimation; for all the other assays, LB broth was used for supernatant preparation. Bacterial cultures were supplemented with F-1 (0.6 mg ml^{-1}, 0.8 mg ml^{-1}, 1 mg ml^{-1}) & rhein (0.15 mg ml^{-1}) and incubated overnight. Post incubation, these tubes were centrifuged (11 180*g* for 10 min). Cell-free supernatants were collected, syringe filtered (Millipore filter; the size of 0.45 μm) in sterile Eppendorf tubes, and maintained at 4 °C for further analysis of virulence factors.

The method previously described by Kessler *et al.* & Shah *et al.*[41,42] was employed for staphylolytic protease quantification. 500 μl culture supernatants of F-1, rhein & AZM were suspended in an equal volume of overnight grown boiled *S. aureus* suspension (prepared in 0.03 M Tris–Cl buffer (pH ∼ 8.5)). Following the incubation, OD_{600} was determined at 0 h and after 3 h of incubation using PerkinElmer UV-Vis Spectrophotometer Lambda 25 model. Enzyme activity was expressed as units per ml, with 1 unit corresponding to a reduction in OD by 0.01.[43]

The elastolytic activity was performed as reported by Adonizio *et al.* & Gala *et al.*[37,44] 500 μl of F-1, and rhein treated culture supernatant was blended with the same amount of Elastin Congo Red (ECR) prepared in 100 mM Tris, and 1 mM $CaCl_2$ (pH = 7.2) containing 10 mg ml^{-1} of ECR (Sigma); this mixture was incubated at 32 °C overnight. Insoluble ECR was removed through centrifugation of the tubes at low speed (5000*g* for 5 min). Elastin Congo Red (ECR) works as a substrate, wherein the elastase enzyme action separates Congo Red from the conjugate, leading to conversion of the insoluble ECR into a soluble form, thereby imparting a red colour to the solution. Thereafter, elastase enzyme levels were assessed in terms of a decrease in enzymatic activity. Decrease in elastase enzyme activity was expressed as units per ml, with 1 unit corresponding to a reduction in OD by 0.01.

Pyocyanin levels were evaluated as per the method of O'Loughlin *et al.*[45] 1 ml of treated (F-1, rhein, and AZM) bacterial culture supernatants were extracted in chloroform (3–5 ml), and the optical density was analyzed at 650 nm. Extracted pyocyanin pigment concentration was calculated using molar extinction coefficient ε = 17.072 ml μg^{-1} cm^{-1}.[46]

Rhamnolipid production was quantified using the orcinol method, as per the method of Koch *et al.*, with some modifications.[47] Culture supernatants of treated (F-1, rhein, AZM) and untreated bacteria were collected, and rhamnolipids in the culture supernatant were extracted using diethyl ether. The rhamnolipid-containing solvent layer was collected and evaporated to dryness. To the above assay, tubes containing dried rhamnolipids were redissolved in distilled water (5 μl) and 450 μl of 0.19% orcinol (in 54% H_2SO_4) solution. This mixture was mixed thoroughly, and it was then boiled at 85 °C for 25 min and cooled down; for every reaction sample, OD was recorded at 421 nm. Rhamnolipid content in the samples was quantified by plotting the standard curve of the rhamnolipid standard.

2.10 Swarm, swim & twitch motility assays

All three motilities in *P. aeruginosa* were determined as per Alain Filloux and Juan-Luis Ramos *et al.*[48–50] Swarm plates were prepared using bacto-agar (0.8%), bacto-peptone (1%), glucose (1%), and NaCl (0.5%), and swim plates were prepared using tryptone (1%), NaCl (0.5%) and agar (0.4%). Different concentrations of F-1 and rhein were added to molten media (cooled at 45 °C), and subsequently solidified. 5 μl inoculum of PAO1 (OD_{600} at 0.2) was inoculated in the centre of the plate. Plates were incubated at 32 °C in the upright position overnight. The decrease in migration was measured by examining the swarm and swim zones (mm).

In a similar way, the twitch plates were prepared. The treated plates were stab inoculated using a sterile toothpick containing *P. aeruginosa* into the bottom of the plates. These plates were then incubated at 32 °C for 18 h, and the twitch zone (interstitial colony) was recorded.

2.11 Effect of test samples on biofilm formation

2.11.1 Biofilm formation assay. The effects of the test sample on biofilm were determined as per the method of Gala *et al.*[37] Dose-dependent concentrations of F-1 (0.6 mg ml^{-1}, 0.8 mg ml^{-1}, and 1 mg ml^{-1}) and rhein (0.15 mg ml^{-1}) were combined with 200 μl of *P. aeruginosa* culture ($OD_{600} = 0.2$) and dispensed into a sterile 96 well microtiter plate. Bacteria treated with AZM (4 μg ml^{-1}) was utilized as the positive control. Biofilms were then grown statically overnight in the 96-well plate. Following incubation, unadhered planktonic bacterial cells were carefully removed after washing with double distilled water and naturally air-dried. Biofilm was fixed for 15–20 min using methanol and then stained with crystal violet dye (0.1%) for 20 min. Later the excess stain was washed off using sterile distilled water. The bacterial cell-bound stain in biofilms was solubilized in 200 μl ethanol (aqueous 96%) and spectrophotometrically analyzed at 590 nm (Epoc2 (BioTek)). The experiments were done in three independent experiments with three replicates.[37,51]

2.11.2 Environmental scanning electron microscopy (e SEM) & confocal laser scanning microscopy (CLMS) for visual analysis of biofilms. The biofilm inhibition property of F-1 and rhein in *P. aeruginosa* was visualized by employing FEI Quanta 200 scanning electron microscope (SEM) as described by Husain *et al.*[24] Overnight grown bacterial culture ($OD_{600} = 0.2$) was mixed with different concentrations of F-1 (0.6–1 mg ml^{-1}), rhein (0.15 mg ml^{-1}) and AZM (4 μg ml^{-1}). 10 μl was withdrawn and grown over the sterile coverslip surface (1 × 1 cm) and kept in a sterile 24-well plate. After overnight incubation at 35 °C, Phosphate Buffer Saline (PBS) (pH = 7.2) was employed to remove un-adhered cells and finally subjected to fixation with glutaraldehyde (2% v/v) for half an hour. These cells on the coverslips were further dehydrated using increasing concentrations of ethanol (30–100%) and allowed to dry. The dried membranes were coated with platinum for 2 min using a sputter-coating system. Finally, biofilms formed on the coverslip surface were observed under a scanning electron microscope (Quanta 200).

Confocal laser scanning microscopy (CLSM) investigation of the test sample treated *P. aeruginosa* was done as reported previously by Singh *et al.* and Shah *et al.*[41,52] For the CLSM analysis, the treated bacterial samples were prepared and incubated the same way as stated for SEM analysis. Following the incubation, slides were carefully washed with phosphate buffer saline (pH ~ 7.2) to detach unadhered bacterial cells, stained with a mixture of SYTO9/propidium iodide, and placed in the dark (15 min). Finally, the cells were visualized under a CLMS microscope. Propidium iodide ($\lambda_{ex}/\lambda_{em}$ 490/635 nm) and SYTO-9 ($\lambda_{ex}/\lambda_{em}$ 480/500 nm) dyes were used for confocal study in a 1 : 2 ratio. CLSM was performed using a CLSM (Zeiss LSM 800, Carl Zeiss, Jena) by keeping the magnification (40×) for capturing the images.

2.12 Quantitative real-time PCR

The expression levels of crucial QS regulatory genes (*lasI*, *lasR*, *rhlI*, and *rhlR*) in the PAO1 strain were analyzed using real-time polymerase chain reaction (qRTPCR).[53] Total cellular RNA was extracted from overnight treated F-1 (0.6–1 mg ml^{-1}), rhein (0.15 mg ml^{-1}), AZM (4 μg ml^{-1}), and untreated culture of *P. aeruginosa* PAO1 (OD_{600} of 0.2) using TRIzol reagent (Thermo Scientific, United States). Purity and total extracted RNA were quantified at 260/280 nm (take 3 plate in Epoc2 by BioTek). From the extracted RNA, single-stranded cDNA synthesis was done using iScript™ reagent kit (BIO-RAD) as given by the manufacturer. The cDNA template amplification was carried out using SYBR® green master mix (Thermo Scientific, USA) and the primers mentioned in ESI Table 2.† Reaction protocol was carried out on the Applied Biosystems Step One Real-Time PCR instrument (California, USA). The reaction program was done as follows: 95 °C for 5 min, denaturation at 95 °C for 15 s, annealing at 55 °C for 30 s, and extension at 72 °C at 30 s for 40 cycles. The melting curve was done as follows: analysis 60 °C to 95 °C, with a rise in temperature of 0.5 °C every 3 s. The housekeeping *rpsL* gene was employed as a reference for normalization of gene expression; the $2^{-\Delta\Delta C_t}$ method was utilised to determine the differential gene expression of the QS-associated genes.[41]

2.13 Effect of test samples on survival of *Caenorhabditis elegans* (*C. elegans*)

2.13.1 *C. elegans* paralytic assay. *C. elegans* culture was maintained as mentioned in ESI (Method 1†). F1, rhein, and AZM were mixed in molten brain heart infusion agar, cooled, and then used for diagnosis of paralysis in worms (35 mm). Following the solidification, 500 μl of an overnight grown *P. aeruginosa* culture (BHI broth 0.2 OD_{600}) was seeded and later incubated (in Hexatech HIPL – 035C) at 31 °C overnight. Untreated worms seeded with *E. coli* OP50 were utilized as negative control plates, while AZM (4 μg ml^{-1}) treated plates were employed as a positive control. Worms in the L-4 stage were washed off thrice using M9 buffer (pH = 6.0 ± 0.2). Then, droplets containing 10–15 synchronized adult worms (L4 stage) were placed on the bacterial lawns to score paralysis hourly for 4–5 h. When the worms stopped responding to physical stimuli, they were declared dead.[44]

2.13.2 *C. elegans* fast-killing assay & slow-killing assay. For the fast-killing assay, specific media – peptone–glucose–sorbitol (PGS) (ESI Table 3†) – was utilized, as given by Miklos *et al.*[54] In contrast, the slow-killing assay was performed in Nematode Growth Medium (NGM) (ESI Table 4†). The rest of the protocol was performed in a similar way as mentioned for the paralytic assay above.[44,55]

2.14 Molecular docking studies

Molecular docking studies further validated the anti-QS potential of main phytoconstituents detected by GC-MS and LC-MS. The present work studied the virtual interaction of the identified constituents with LasI and LasR using AutoDock4 software.[56,57] 3D structures of LasI and LasR were acquired from the RCSB Protein Data Bank (PDB code: 1RO5 and 2UV0, respectively).[58] These protein structures were checked and prepared with their consistency and charges in AutoDock4. Kollman charges were added to the protein, and final structures were saved in *. PDBQT format. The active site receptor grid was generated on the protein structure. 50 docking experiments were conducted using the Lamarckian genetic algorithm to determine the binding energy (docked energy) for the ligand–protein complex. The maximum number of energy evaluations of 25 million was applied for each docking experiment. All the identified phytocompounds from the GC-MS study were virtually built using the Marvin sketch tool and converted to *. PDBQT format by using the Open Babel software. These small molecular structures were then used for docking study in AutoDock4 to understand the interactions with LasI and LasR. All the 3D ligand–receptor interaction images were generated using the Chimera tool,[59] and 2D interaction images were generated using Discovery Studio Visualizer.

2.15 Statistical analysis

All the experiments were validated by performing in triplicate ($n = 9$) for three consecutive days. The graphs were plotted using GraphPad Prism software (version 5.0; GraphPad Software, Inc., USA). All values presented in the results are an average of 3 independent experiments. Differences between groups were compared using a one-way analysis of variance followed by Dunnett's *post hoc* test, with a *P*-value of ≤ 0.05 being considered significant. Killing curves represent the mean value of three independent experiments.

3. Results and discussion

3.1 Fraction collection and pooling

From the flash chromatography, four fractions were collected, dried, and reconstituted in DMSO. These fractions were stored at 4 °C for subsequent analysis.

3.2 Fraction based anti-QS activity (short-chain AHL inhibition assay)

The effectiveness of fractions and their most crucial constituent rhein was analyzed using sensor strain *C. violaceum* 12472. Purple pigment production of *C. violaceum* 12472 is controlled by CviIR dependent circuit, and the loss of pigment production suggests the obstruction in the QS pathway.[60] As shown in Fig. 2B, fraction-1 (F-1), at various concentrations of 0.4 mg ml^{-1}, 0.6 mg ml^{-1}, 0.8 mg ml^{-1}, and 1 mg ml^{-1}, showed a clear zone of pigment inhibition of 11.0 ± 1.1, 13.1 ± 0.9, 14.3 ± 2, and 17.9 ± 1.6 mm respectively around the wells. Fraction-2 showed the zone of bactericidal activity; fraction-3 and fraction-4 showed no noticeable pigment inhibition at lower concentrations (Table 1). In an independent assay, DMSO showed no pigment inhibition around the well, while AZM displayed 18.9 ± 0.5 mm of the zone (ESI Fig. 2†). From the initial screening, fraction-1 showed the best anti-QS activity. Rhein exhibited a zone of pigment inhibition of 10.0 mm ± 0.8 mm, 12.9 ± 1 mm, 13.5 ± 2.2 mm, and 17.2 ± 2 mm at concentrations of 0.025 mg ml^{-1}, 0.05 mg ml^{-1}, 0.1 mg ml^{-1}, and 0.15 mg ml^{-1} respectively. These results directly corroborate the work that showed violacein pigment inhibition of *C. violaceum* by mango plant extract and clove oil from *Aeromonas hydrophila.*[24,61] A comparative study of F-1 and rhein was done for other QS-mediated assays.

3.3 Analysis of phytochemical of F-1

3.3.1 GC-MS results. The major compounds identified in fraction 1 by gas chromatography-mass spectrometry (GC-MS) displayed the presence of 14 volatile oils and fatty acids, as shown in the chromatogram (Fig. 3) and Table 2. Similarly, in the study of Kulkarni *et al.*, crude methanolic extract of *Cassia fistula* (found to contain a total of ten different phytoconstituents) was identified from GC-MS and showed vitro anticancer activity in human prostate cancer cell line.[62]

3.3.2 LC-MS linearity and the limits of detection and quantification. Multiple reaction monitoring (MRM) chromatogram of standard rhein and rhein in F-1 showed the same retention time of 2.5 min as shown in Fig. 4A-1 and A-2. The linearity of the calibration curves was determined and analyzed with standard rhein of concentrations ranging from 32 to 2500 ng ml^{-1} in F-1 (Fig. 4B-1 and B-2). A calibration curve was plotted for each concentration, comparing the peak area ratio to the internal standard. The results demonstrated linearity of 32–2500 ng ml^{-1} for rhein in F-1 with correlation coefficients (r^2) > 0.998 obtained for the regression lines.[63]

3.4 Effect of F-1 and rhein on *P. aeruginosa* growth

The growth curve analysis of *P. aeruginosa* PAO1 in the presence of different concentrations of F-1 (0.6–1 mg ml^{-1}) & rhein (0.15 mg ml^{-1}) showed no inhibitory effect on bacterial cells compared with the control group (untreated *P. aeruginosa*). PAO1 attained a stationary phase after 8 h incubation. Incubation of bacteria with AZM did not significantly affect the bacterial growth curves. Conventional antibiotics hamper the crucial metabolic process of bacterial cells and exert tremendous selection pressure on bacterial cells, leading to the evolution of MDR strains.[64] Our growth curve assay results confirmed that F-1 and rhein at various concentrations did not show growth inhibition of *P. aeruginosa* (Fig. 5A). This finding goes well with the research

Table 1 Anti-QS and antibacterial activity of various collected fractions and standard rhein

	Fraction-1 (mg ml^{-1})				Fraction-2 (mg ml^{-1})				Fraction-3 (mg ml^{-1})				Fraction-4 (mg ml^{-1})				Rhein (R) (mg ml^{-1})			
Activity	0.4	0.6	0.8	1	0.4	0.6	0.8	1	0.4	0.6	0.8	1	0.4	0.6	0.8	1	0.025	0.05	0.1	0.15
Anti-microbial activity	−	−	−	−	+	+	+	+	−	−	−	−	−	−	−	+	−	−	−	−
Anti-QS activity	+	+	+	+	−	−	−	−	+	+	+	+	+	+	+	+	+	+	+	+

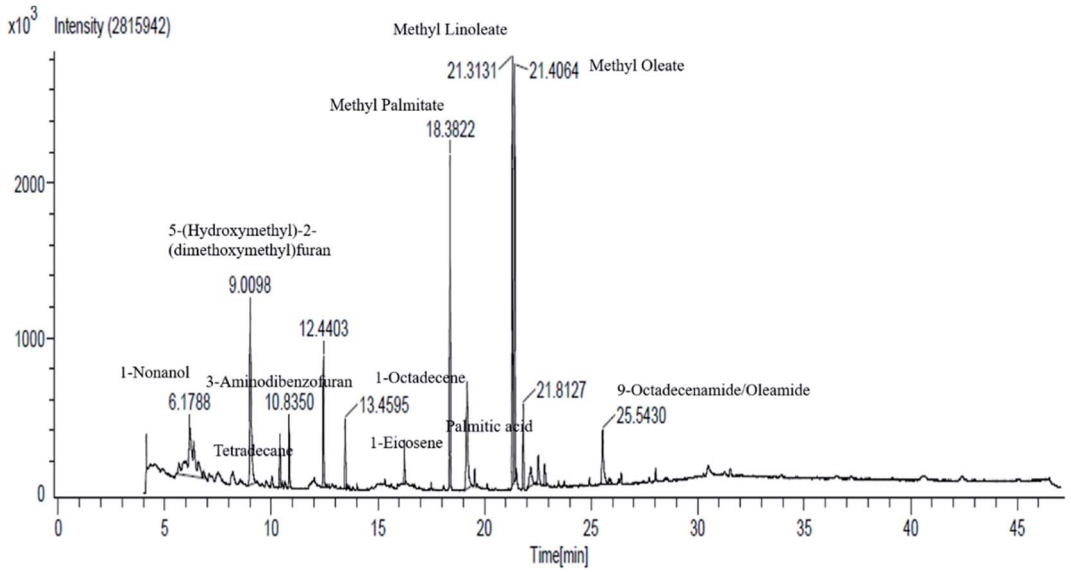

Fig. 3 GC-MS analysis of fraction-1 of *Cassia fistula* fruit pods.

results of Kalia *et al.*, in which parthenolide at 1 mM showed no growth inhibitory effects on bacterial growth.[65]

3.5 Quantitative evaluation of violacein inhibition

In the spectrophotometric quantitative detection method, violacein pigment production was reduced by approximately 26 ± 0.8%, 39 ± 0.6%, and 63.4 ± 0.4% at dose-dependent concentrations of 0.6 mg ml^{-1}, 0.8 mg ml^{-1}, and 1 mg ml^{-1}, respectively, by F-1 (Fig. 5B). Rhein alone manifested approximately 13 ± 1%, 24 ± 0.9%, and 43 ± 0.7% inhibition of violacein production at 0.5 mg ml^{-1}, 1 mg ml^{-1}, and 0.15 mg ml^{-1} concentrations, respectively; it was statistically significant then untreated control. These results validate the QS inhibitory role

Table 2 Identification of phytochemicals in purified fraction-1 of *Cassia fistula* using GC-MS analysis

Peak number	Compound name	Time (min)	Class
1	1-Nonanol	6.18	Volatile oil component
2	5-(Hydroxymethyl)-2-(dimethoxymethyl)furan	9.00	Volatile oil components
3	Tetradecane	10.39	Volatile oil components
4	3-Aminodibenzofuran	10.83	Volatile oil components
5	2,4-Di-*tert*-butylphenol	12.43	Class of phenols
6	1-Octadecene	13.45	Plant fat
7	1-Eicosene	16.23	Long-chain primary fatty alcohol
8	Methyl palmitate	18.37	Fatty acid methyl ester
9	Palmitic acid	19.17	Saturated long-chain fatty acid
10	Methyl linoleate	21.31	Linoleic acid
11	Methyl oleate	21.40	Fatty acid methyl ester
12	Methyl stearate	22.17	Fatty acid methyl ester and octadecenoate ester
13	Dihydrorhodamine/palmitic acid	22.52	Saturated fatty acid
14	Methyl linoleate	22.81	Linoleic acid
15	9-Octadecenamide/oleamide E	25.54	Fatty amide derived from oleic acid

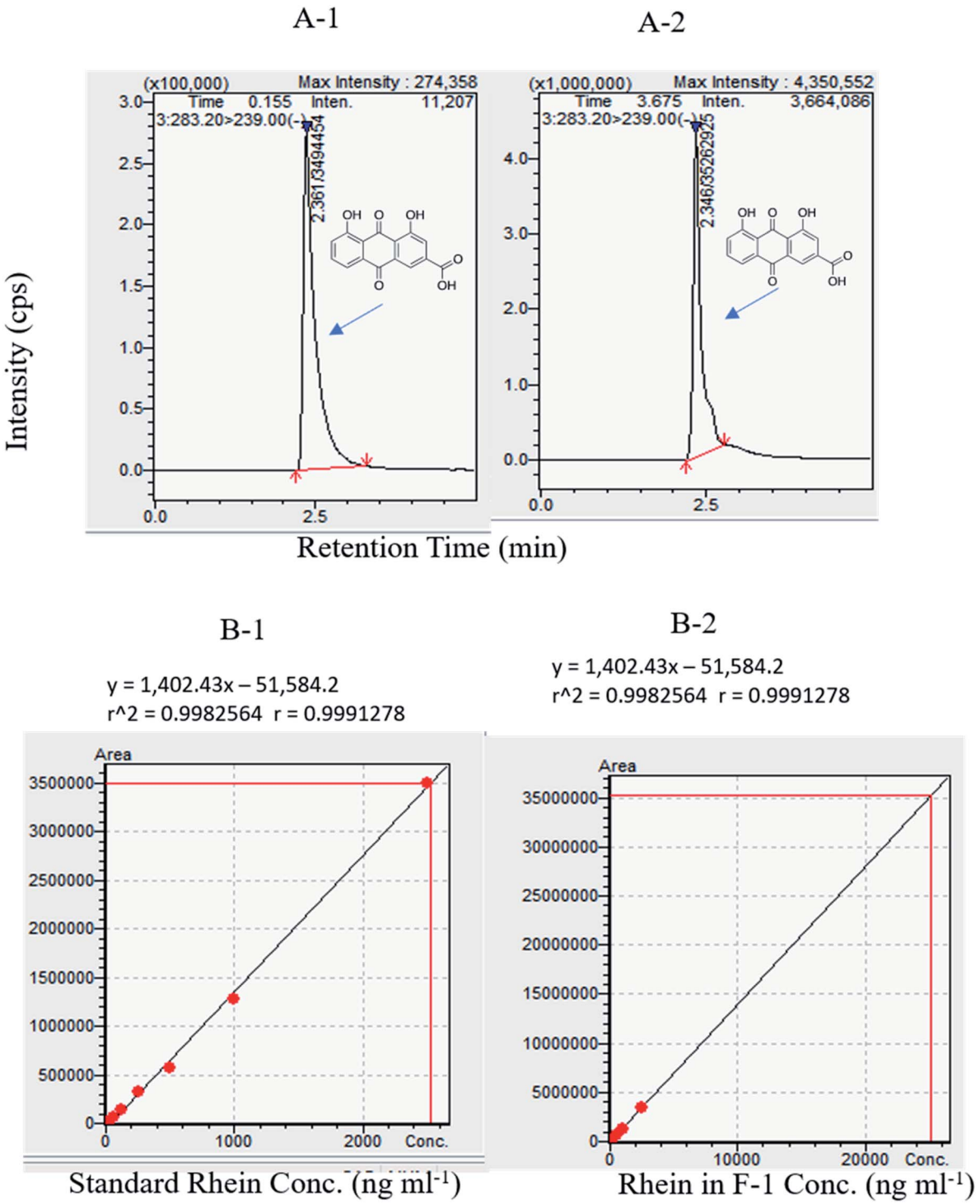

Fig. 4 (A-1) Typical MRM chromatogram of standard rhein RT: 2.5 min. (A-2) Rhein in F-1 (287.4 ng ml^{-1}) RT: 2.5 min. Rhein linearity results using LC-MS. (B-1) Standard rhein at various concentrations *viz.* 32 ng ml^{-1}, 64 ng ml^{-1}, 125 ng ml^{-1}, 250 ng ml^{-1}, 500 ng ml^{-1}, 1000 ng ml^{-1}, 2500 ng ml^{-1} (B-2) F-1 at various concentrations of rhein in F-1 *viz.* 32 ng ml^{-1}, 64 ng ml^{-1}, 125 ng ml^{-1}, 250 ng ml^{-1}, 500 ng ml^{-1}, 1000 ng ml^{-1}, and 2500 ng ml^{-1}.

of F-1 and rhein in rhlI/R circuitry of *P. aeruginosa*. The result is in line with the data of Aswathanarayan *et al.*, in which berberine was screened using the biosensor bacteria *C. violaceum.* Berberine reduced violacein production in the wild-type strain by 62.67% at a concentration of 1.6 mg ml^{-1}.[66]

3.6 Long-chain AHL inhibition assay

The level of 3-oxo-C12 HSL in F-1 and rhein treated *P. aeruginosa*, was detected using reporter strain *E. coli* MG4/pKDT17. The AHL levels in the supernatant of the F-1 treated sample was reduced by

21.2%, 47.7%, and 68.9% at 0.6 mg ml^{-1}, 0.8 mg ml^{-1}, and 1 mg ml^{-1}, respectively; this indicates that different fraction concentrations (F-1) significantly target the las IR circuit. The extent of inhibition by standard rhein was 24.9%, 35.3% and 56.4% at concentrations of 0.05 mg ml^{-1}, 0.1 mg ml^{-1} & 0.15 mg ml^{-1} respectively. AZM showed around 78.72% reduction in β galactosidase production (Fig. 5C). Similarly, a dose-dependent reduction in AHL levels in *P. aeruginosa* was recorded upon treatment with eugenol, and *Mangifera indica* extracts.[61,67]

3.7 Effect of F-1 & rhein on bacterial virulence factors

Both *Las*I/*Las*R and *Rhl*I/*Rhl*R circuits conjointly regulate the array of virulence factors throughout the advancement of infections in the host. These virulence factors *viz.* LasB elastase, LasA protease, pyocyanin, rhamnolipids, and I flagella type IV pili govern the pathogenicity of bacteria PQS.[68] The BHL (Butyryl Homoserine Lactone) and OdDHL (*N*-3-oxo-dodecanoyl homoserine lactone) signal control LasB elastase, LasA protease, and alkaline protease production. LasA and LasB are crucial players in the deterioration of matrix proteins and the degradation of the host tissues.[69]

Our data showed that with increasing concentrations of F-1 (0.6 mg ml^{-1}, 0.8 mg ml^{-1} and 1 mg ml^{-1}), protease activity reduced significantly ($p < 0.01$) by 28%, 43% and 56% respectively, whereas AZM showed 74% protease activity inhibition (Fig. 6A). Rhein (0.15 mg ml^{-1}) showed a profound effect in reducing protease activity by 64.

Similarly, LasB elastase is a multifunctional metalloenzyme that is highly potent. It plays an important role during host cell infection and can inactivate various biological tissues and immunological agents. On exposure to F-1 (0.6 mg ml^{-1}, 0.8 mg ml^{-1}, 1 mg ml^{-1}), there was a noticeable reduction in LasB elastase by 27%, 51% and 68% respectively (Fig. 6B). Rhein (0.15 mg ml^{-1}) showed a substantial effect with a 75% decrease in the elastase activity, almost equal to positive control AZM (77.1%).

Pyocyanin is a blue, green cytotoxic factor released in copious amounts during cystic fibrosis lung infection. QS

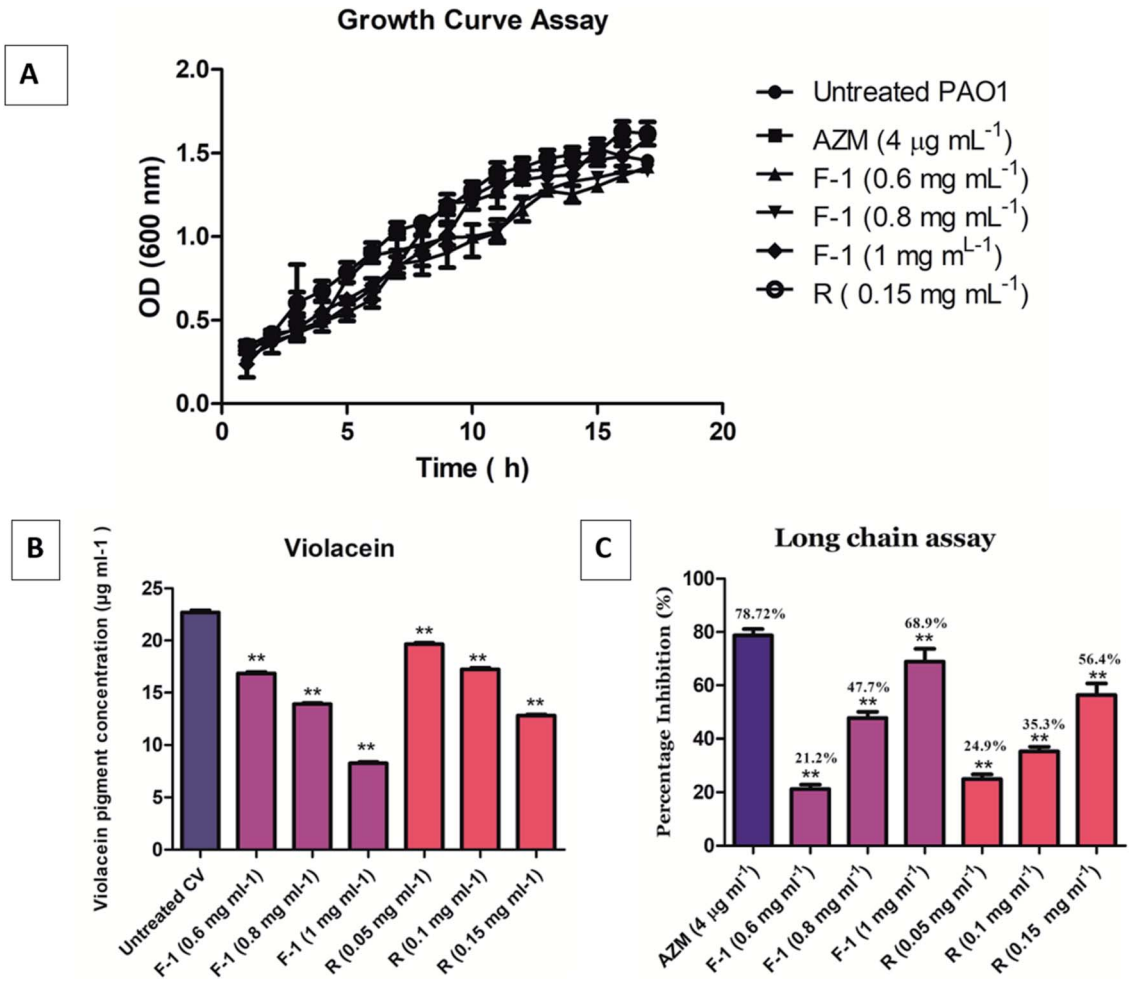

Fig. 5 (A) *P. aeruginosa* growth curve acquired on treatment with F-1, rhein (R) and AZM. (B) Quantitative assessment of F-1 and rhein on violacein pigment inhibition in *C. violaceum* 12472. *Y* axis represents the decrease in reduction in violacein pigment concentration. Data is shown as average of triplicate readings with SD represented as bar where ** indicates $p \leq 0.05$ with respect to untreated control. (C) 3-Oxo-C12 HSL production inhibition, which is quantified using bioreporter strain *E. coli* pkdt17. Mean values of three triplicate independent experiments ($n = 9$) and SD are presented.

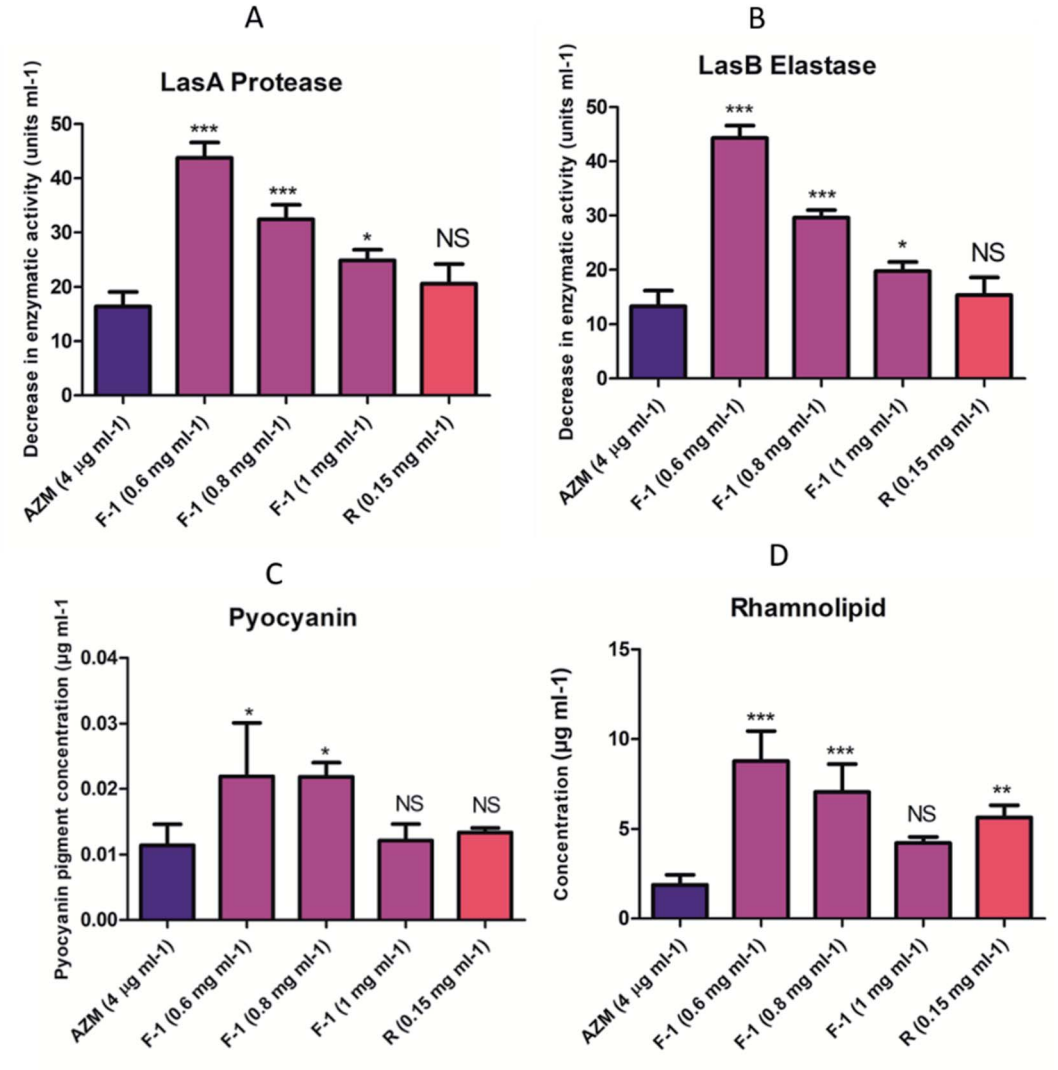

Fig. 6 Effect of F-1, Rhein and AZM on the virulence factor of culture supernatant (A) LasA proteolytic activity, (B) LasB elastolytic assay (C) pyocyanin assay (D) rhamnolipid assay. The bars indicate the standard deviation for triplicate sets of experiments. The three independent experiments were performed in triplicate ($n = 9$), and values were shown as the average of three independent experiments compared with control AZM (**$p < 0.05$, ***$p < 0.001$).

controls the production and secretion of pyocyanin. We investigated the effects of various concentrations of F-1 and rhein on the potential of *P. aeruginosa* to synthesize and secrete pyocyanin. Pre-treatment with F-1 concentrations of 0.6 mg ml^{-1}, 0.8 mg ml^{-1}, and 1 mg ml^{-1} displayed 48%, 55% and 59% pyocyanin reduction respectively (Fig. 6C). The extent of pyocyanin production was lowered by 72% upon treatment with rhein (0.15 mg ml^{-1}), comparable with the decline observed with AZM (78%). The depletion in pyocyanin levels indicates the potential effects of test samples on the QS circuit of *P. aeruginosa*.

Rhamnolipids play a critical role in biofilm formation and bacterial pathogenesis by modulating the swarming motility. The efficacy of F-1 and rhein in reducing the secretion of rhamnolipids was quantified. As shown in Fig. 3, dose-dependent concentrations of F-1 (0.6 mg ml^{-1}, 0.8 mg ml^{-1}, and 1 mg ml^{-1}) showed 41%, 54%, and 70% reduction in rhamnolipid production respectively. At 1 mg ml^{-1} of F-1, the inhibition was far better than AZM. Rhein, a strong constituent of F-1, also showed a 43% decrease in rhamnolipid production (Fig. 6D).

F-1 and rhein treated bacterial supernatant was also tested for all the above virulence assays and showed a remarkable reduction in the virulence factor production. These results are consistent with the study of Luo *et al.* and Zhou *et al.*, in which baicalein and phillyrin showed a varying level (between 10–90%) of virulence factor reduction in *P. aeruginosa*.[22,33]

3.8 Swarm, swim & twitch motility assays

Biofilm forming capacity in *P. aeruginosa* is highly associated with motility. This bacteria displays three types of motility – swarming, swimming (controlled by bacterial flagellar movement), and twitching (controlled by type IV pili) – which play

a fundamental role during various stages of biofilm formation.[70] Therefore, reducing migration movement with plant fraction reflects the decline in biofilm development by interrupting AHL mediated QS mechanism.

The effect of F-1 and rhein on all the three motilities of *P. aeruginosa* was assessed by inoculating overnight cultures of *P. aeruginosa* onto the sample (F-1 and rhein) treated motility plates. As shown in Fig. 7i and ii, a significant reduction in all three motilities was observed. Untreated *P. aeruginosa* PAO1 exhibited 30 mm and 47 mm of swarming and twitching migration zones, respectively. Concentration-dependent dosage of F-1 (0.6 mg ml^{-1}, 0.8 mg ml^{-1} and 1 mg ml^{-1}) resulted in significant decrease ($P < 0.05$) in both swimming and swarming motility by (12.7 mm, 10 mm and 7 mm) & (33 mm, 27 mm and 24 mm) respectively. These reductions were comparable with AZM, which showed a 9.25 mm diameter for swarming and 26 mm for swimming agar plates. Treatment with rhein at 0.15 mg ml^{-1} exhibited 7 mm swarming and 26 mm swimming migrations.

P. aeruginosa PAO1 inoculated plates at various doses (0.6 to 1 mg ml^{-1}) of F-1 showed poor twitch motility (28.3 to 21.9 mm) zones; rhein (0.15 mg ml^{-1}) also imposed the inhibitory effect on type IV pili mediated twitching motility (21.7 mm). Negative control (untreated PAO1) showed great twitching migration of 49.5 mm. However, AZM displayed a significant reduction of 17.4 mm twitching motility of the test pathogen. Pyocyanin is a blue-green toxic pigment produced by bacteria. It is a prerequisite for immune circumvention. In addition, rhamnolipid, a biosurfactant, helps initiate biofilm colonization and spread in host tissue.[71] In conclusion, virulence factors production, which is necessary during the host invasion in the early and late stages of infection, is controlled by QS systems; these factors influence the host cellular proteins in the infected tissues and aid bacterial invasion and growth. A similar reduction in motilities was reported by Zhou *et al.* & Aleksic *et al.*[72,73]

Hordenine treatment significantly reduced tendril formation and colony diameter in swimming and swarming motility at concentrations varying from 0.5 mg ml^{-1} to 1.0 mg ml^{-1}. Aleksic *et al.* showed that various synthetic derivatives of *N*-octaneamino-4-aminoquinoline effectively inhibited swimming, swarming and twitching motilities.

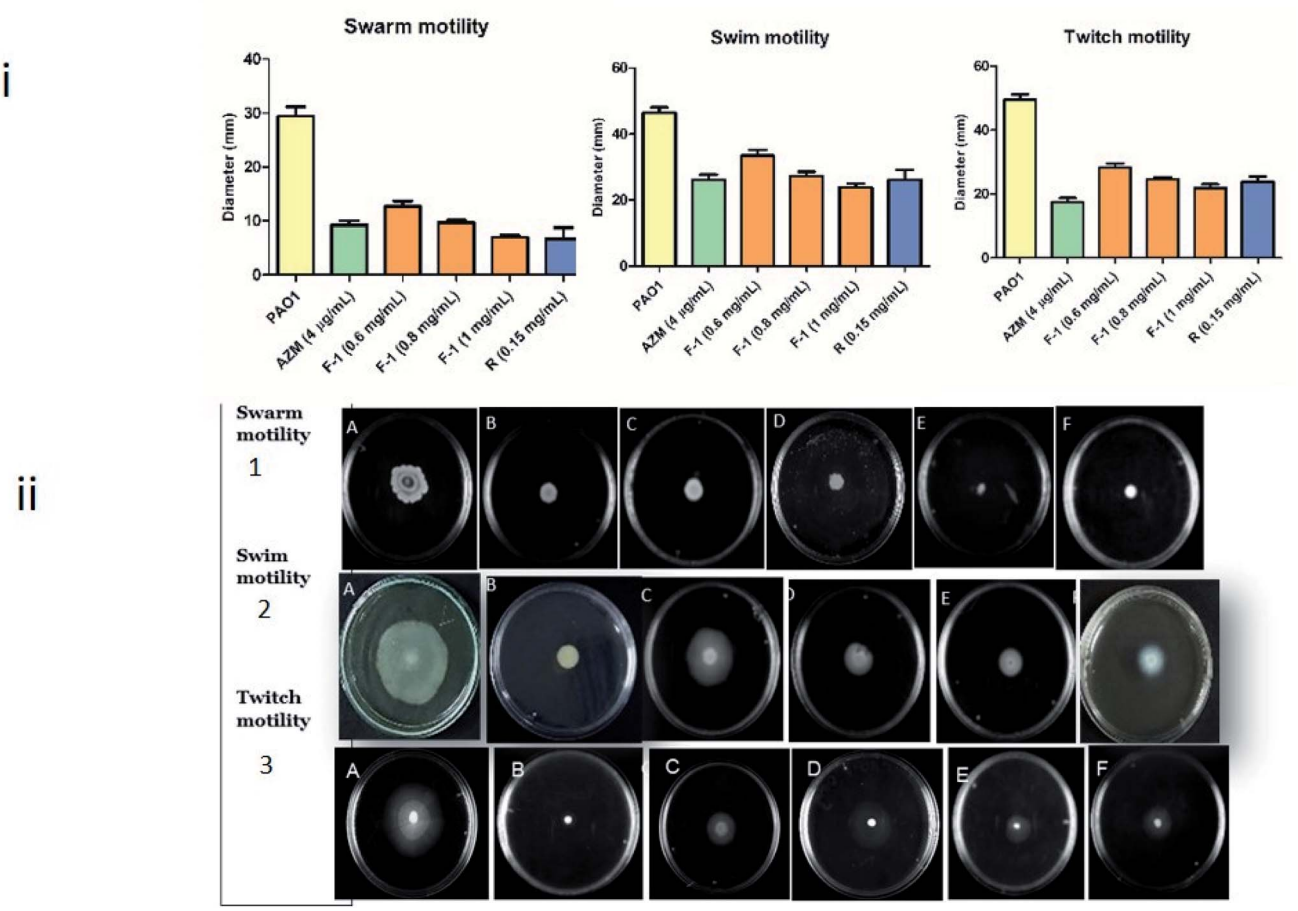

Fig. 7 Motility inhibition of *P. aeruginosa* by treatment of F-1, rhein and AZM (i) graphical representation of (1) swarming, (2) swimming and (3) twitching motility of *P. aeruginosa* (ii) pictorial representations of (1) swarming, (2) swimming and (3) twitching motility of *P. aeruginosa*. In all three panels *viz.* 1, 2 and 3, plate (A) represents untreated *P. aeruginosa*, plate (B) represents AZM treated *P. aeruginosa*, and plates (C), (D) and (E) represent *P. aeruginosa* treated with F-1, at 0.6 mg ml^{-1}, 0.8 mg ml^{-1} and 1 mg ml^{-1}, respectively. Plate (F) in all three panels represents rhein treated *P. aeruginosa*. Results are shown as mean of three (swarming, swimming & twitching) independent experiments ($n = 9$).

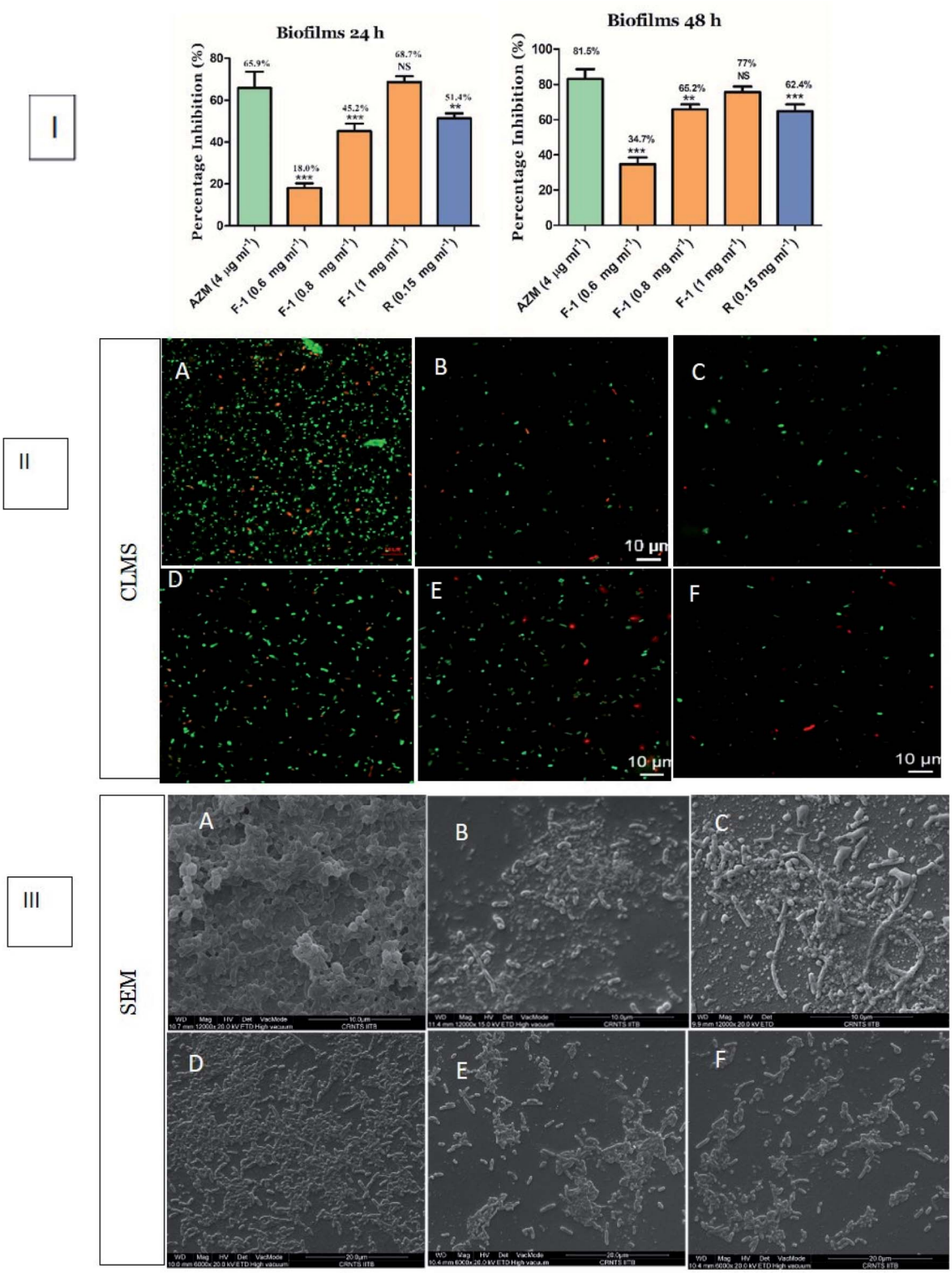

Fig. 8 Biofilm inhibition assay (I) quantitative assay representing the effect of F-1, rhein on *P. aeruginosa* PAO1 biofilm after 24 h of incubation (II) confocal laser scanning microscopy images of *P. aeruginosa* PAO1 biofilms (III) scanning electron microscopic images of *P. aeruginosa* biofilms where (A) untreated *P. aeruginosa* (B) AZM (4 μg ml^{-1}), (C) rhein (0.15 mg ml^{-1}) and (D–F) F-1 treatments at concentrations of 0.6 mg ml^{-1}, 0.8 mg ml^{-1} and 1 mg ml^{-1}. The asterisk above the bars indicate statistically significant difference compared to AZM (**p < 0.05; ***p < 0.001).

3.9 Effect on biofilm formation

Depending on the above affirmation, we further determined the effect of F-1 and rhein on biofilm formation. *P. aeruginosa* is popular for its biofilm-forming property, which is controlled by the *rhl* circuit. In biofilms, bacteria live in the sessile community encased in Extracellular Polymeric Substance (EPS). They

tend to adhere to various surfaces and initiate bacterial colonies, leading to severe chronic infections in immunocompromised patients that are difficult to eradicate.[74]

Conventional crystal violet (CV) binding assay was performed to analyze the effect of F-1 and rhein on biofilm formation. The spectrophotometric analysis showed an 18–69% decrease in bacterial biofilm production in a concentration-dependent manner of F-1 (0.6–1 mg ml^{-1}), as shown in Fig. 8I. The lowest concentration of F-1 exhibited comparatively less inhibition of biofilm biomass by 18%; however, F-1 at 1 mg ml^{-1} concentration demonstrated 69% inhibition which was more significant than AZM (66%). Similarly, treatment with rhein showed 51.4% inhibition of the biofilm formation of *P. aeruginosa* PAO1. Further, the effect of F-1 and rhein was analyzed using confocal microscopy and scanning electron microscopy. Microscopy analysis was performed to validate quantitative biofilm inhibition data and give a visual representation of biofilms. In confocal laser microscopy (CLMS) imaging analysis, the density of planktonic cells was notably reduced with increasing dosage of F-1. Rhein and AZM treated cells showed a decrease in the cell biomass on a glass coverslip. However, the untreated cultures of *P. aeruginosa* build a mat-like thick and dense biofilm on glass coverslips, as shown in Fig. 8II.

Moreover, visualization of the fraction-treated biofilms through scanning electron microscopy revealed a potent reduction in microbial adherence and a scattered appearance of biofilms. As shown in Fig. 8III, the biofilm of the control group (untreated cells) showed excellent adhesion. An entire coverslip was covered with the fully grown biofilm, whereas the exposure of F-1 & rhein led to a drastic reduction in biofilm. These results indicate that rhein-rich F-1 and pure rhein potentially inhibited the biofilm adhesion and further blocked the advancement in the biofilm-forming capacity of *P. aeruginosa*.

In the current study, upon treatment of *P. aeruginosa* with F-1 (1 mg ml^{-1}) and rhein, we observed a significant diminution in biofilm biomass in *P. aeruginosa* PAO1 in 96 well plates without compromising bacterial growth. Major constituent rhein also reduces biofilm thickness, resulting in the scattered pattern of bacteria on the glass coverslip. These research results are in conformity with Rajkumari *et al.* and Zhou *et al.*[72,75]

3.10 Expression of QS-regulated genes

lasI, *lasR*, *rhlI*, *rhlR* are vital regulators of the QS-regulated circuit and play an indispensable role in QS-related virulence factors production and biofilms development.[76] These QS-regulated key genes were analyzed using qRTPCR for treated (F-1, rhein, and AZM) and untreated *P. aeruginosa* PAO1 (control). The relative expression of QS-regulated genes – *lasI*, *lasR*, *rhlI*, *rhlR* – was determined by calculating C_t values. *RpsL* gene was employed as a reference gene. Melting curves acquired for all the genes (*rpsL*, *lasI*, *lasR*, *rhlI*, and *rhlI*) showed that control and treated samples of *P. aeruginosa* had the same melting profile, and no primer dimer was monitored (data not shown). Relative expression of treated test samples was compared with untreated bacterial cultures, and the data was analyse using the $2^{-\Delta\Delta C_t}$ method. As stated in real-time PCR data, the highest non-growth inhibitory concentrations of F-1 (1 mg ml^{-1}) showed maximum inhibition in *rhlI* gene while other genes manifested modest inhibition. Rhein-treated *P. aeruginosa* (0.15 mg ml^{-1}) significantly down-regulated the expression levels of *lasI*, *lasR*, *rhlI*, and *rhlR* by 76.5%, 39.5%, 63.5% and 33%, respectively. Results acquired in this study manifested that rhein selectively down-regulates the functions of all 4 genes (Fig. 9A). Similarly, exposure to AZM (positive control) also caused a significant and selective downregulation of the expression of *lasI*, *lasR*, *rhlI*, and *rhlR* by 85.5%, 66%, 49%, and 62.5%, respectively, which is comparable with the results obtained by F-1 and rhein. Overall, F-1 and its main constituent drastically reduced all four gene expression levels in *P. aeruginosa*.

These results indicate that multiple components of F-1 play an essential role in the QS circuit. The study results are in line with the work of Taha *et al.*, in which they showed varying levels of reduction in *lasI*, *lasR*, *rhlI*, and *rhlR* genes upon the treatment with two synthetic peptides (LIVRHK and LIVRRK) in *P. aeruginosa*.[77]

3.11 Effect on the survival of the worms

3.11.1 *Cassia fistula* active fraction & rhein rescue *Caenorhabditis elegans* from paralytic killing, slow killing & fast killing by *P. aeruginosa*. We further investigated the anti-virulence and preventive effects of F-1 and rhein on the ability of *P. aeruginosa* PAO1 to kill *C. elegans*. Paralysis in *C. elegans via P. aeruginosa* PAO1 occurs because of cyanide asphyxiation. Cyanide production in *P. aeruginosa* PAO1 is under the control of HCN operon, operated by the QS regulators, *Las*R and R*hlR*. The high survival rate of worms reflects the inhibitory effect of F-1 and rhein on the QS circuit and bacterial pathogenesis. Treatment with F-1, rhein, and AZM significantly increased the survival rate of infected worms by 70%, 60%, and 80%, respectively, as shown in Fig. 9B.

In slow killing, the assay utilizes low osmolarity media, and the killing of worms occurs over several days. Death of worms happens due to ingestion and aggregation of *P. aeruginosa* in *C. elegans* gut. Subsequently, the infection is controlled by the QS. As shown in Fig. 9C, in the slow killing assay, 60–67% of worms died on *P. aeruginosa* PAO1 treated plate between 48 to 50 h, with the highest concentrations of F-1 (1 mg ml^{-1}), increasing the survival rate significantly by 53% at the end of 72 h incubation. Upon treatment with rhein and AZM, the survival rate was recorded at 60% and 69%, respectively.

On the other hand, phenazine is a crucial virulence factor that plays an indispensable role in the fast killing of *C. elegans* and is partially controlled by the QS circuitry. Fast-killing assay results are depicted in Fig. 9D. Upon exposure to F-1 and rhein, there was a drastic increase in the worms' survival rate by 60% and 57%, respectively, after 5 h. The study results suggest that the addition of F-1 and rhein remarkably increased the survival rate of *P. aeruginosa* PAO1 infected *C. elegans*. Our research results are encouraging and support the results of the previous work in which *Murraya* essential oils at 0.3 v/v concentration significantly increase the survival rate of worms.[78,79]

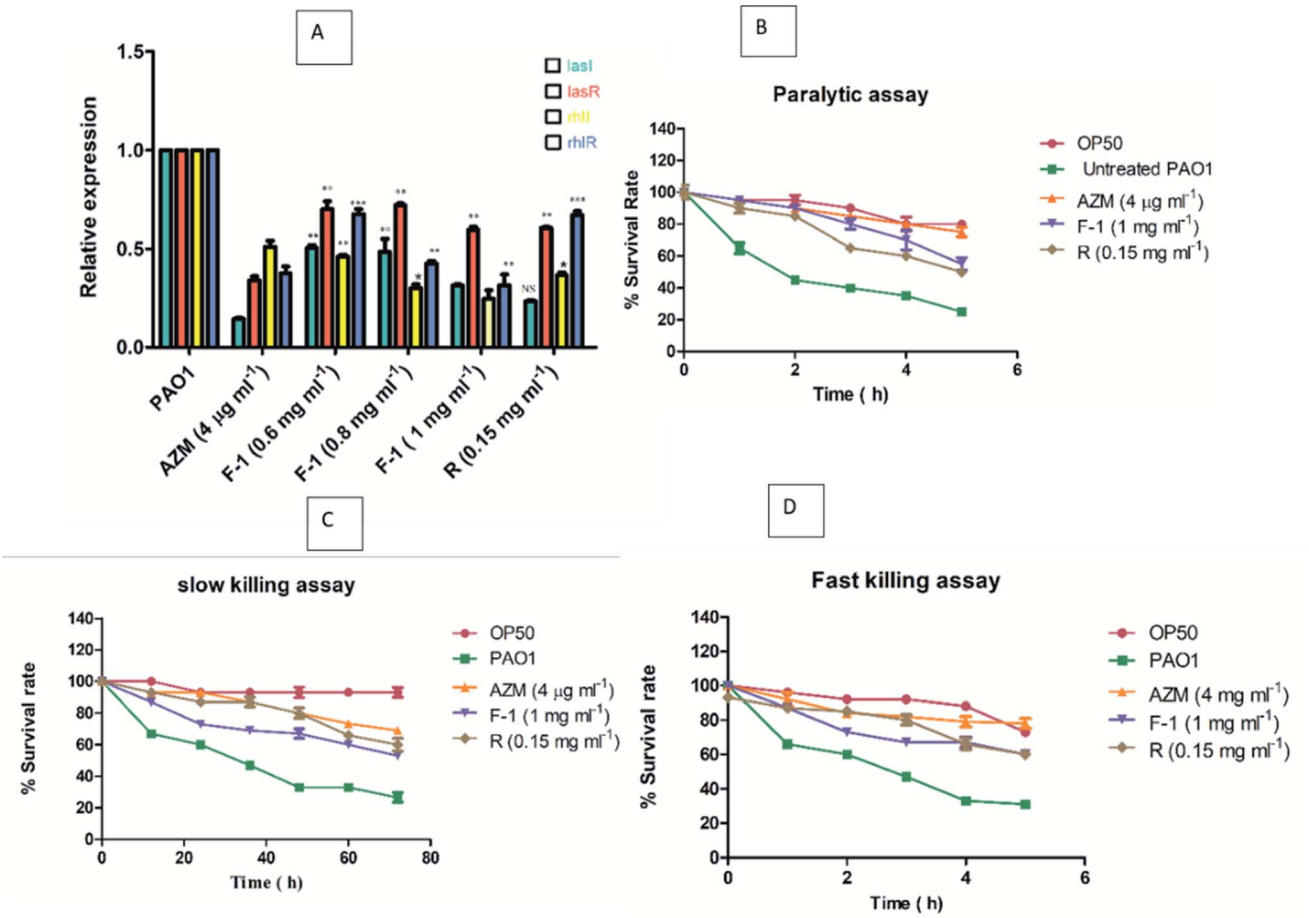

Fig. 9 (A) Bar graph showing expression level of various QS regulatory genes *lasI*, *lasR*, *rhlI*, and *rhlR* genes in *P. aeruginosa* post treatment with F-1 (0.6–1 mg ml^{-1}) and rhein (0.15 mg ml^{-1}). Untreated bacterial culture was used as negative control, while AZM (4 μg ml^{-1}) treated bacterial group was used as positive control. Data represented as the average of three independent experiments and indicated in terms of relative expression with respect to untreated control group. (B–D) Effect of F-1 and rhein on the life span of *Caenorhabditis elegans* where (B) represents paralytic assay (C) slow-killing assay and (D) fast-killing assay.

3.12 Molecular docking study

The molecular docking interactions of all the constituents identified by GC-MS and LC-MS analysis, including rhein, were studied against *LasI* and *LasR* protein structures using AutoDock4. The observed binding energy scores are mentioned in ESI Table 5.† Based on binding scores, it was observed that constituents like rhein, 3-aminodibenzofuran, 5-(hydroxymethyl)-2-(dimethoxymethyl)furan, dihydrorhodamine have an equal affinity towards both the targets under study, *i.e.*, *LasI* and *LasR* receptors. On the other hand, certain constituents like 9-octadecenamide, 2-aminononadecane, methyl stearate, and methyl linoleate showed more affinity towards *LasR* than *LasI*. Phytocompounds of F-1 exhibiting the highest affinity, including rhein, are discussed here. The remaining constituents exhibited almost similar (moderate to less) affinity towards both targets.

The carboxylic acid functionality of rhein stabilizes the *LasI* receptor–ligand complex by strong hydrogen bond interaction with Phe105 and a stable salt bridge with Arg104. The 9-carbonyl functional group of 9,10-dioxoanthracene ring provides additional stability to the complex by creating a hydrogen bond with Thr144. Apart from these interactions, the structure is well stabilized in the receptor active site. Here the 4,5-diOH and 10-carbonyl polar functionalities are aligned with the essential positively charged polar amino acids such as Lys28, Arg30, and Lys31. The aromatic rings of the scaffold are further stabilized by pi–pi stacking interaction with Phe27 and Trp33, along with pi–alkyl interaction with Val148. The interaction of Rhein with the active site of *LasI* is shown in Fig. 10A. The 3-aminodibenzofuran exhibited promising interactions with the active site of *LasI* as shown in Fig. 10B. One of the benzene rings of the scaffold comfortably fits into a hydrophobic pocket comprising nonpolar amino acids like Phe105, Ala106, Val148, Met151, and Met152 Phe117 pi–pi interaction.

Further, the aromatic rings of the scaffold also exhibited pi–alkyl interaction with Val26 and Val148. The oxygen of the furan ring of the scaffold supported ligand–receptor complex stability by establishing a hydrogen bond with Ile107. Similarly, 5-(hydroxymethyl)-2-(dimethoxymethyl) furan also showed promising interactions with *LasI* (Fig. 10C). The 5-

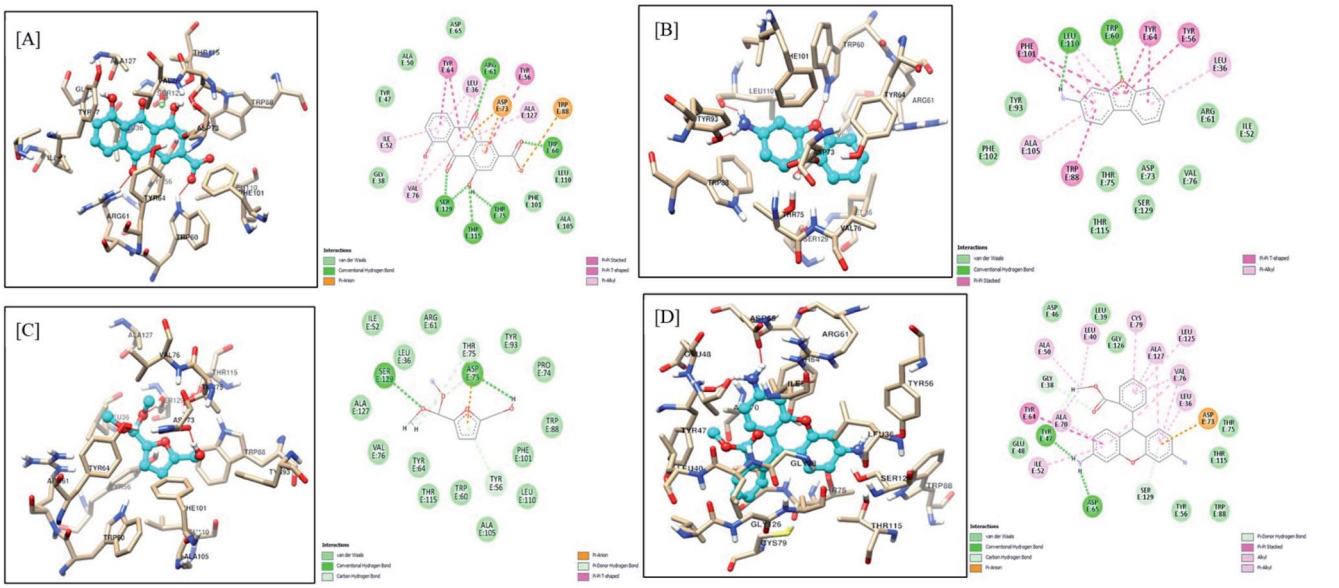

Fig. 10 Docking model of compounds identified by GCMS (A) rhein, (B) 3-aminodibenzofuran, (C) 5-(hydroxymethyl)-2-(dimethoxymethyl)furan and (D) dihydrorhodamine with LasI (PDB ID: 1RO5).

hydroxymethyl group of scaffolds prominently stabilized the complex by forming a hydrogen bond with Arg104, Phe105, and Val143. The furan ring of the scaffold is found to be stabilized between Phe27 and Trp33 aromatic amino acids by pi–pi stacking interaction. Dihydrorhodamine derivative (Fig. 10D) showed promising interaction with *LasI*. The methyl benzoate moiety of the scaffold exhibited encouraging pi–pi interaction with Trp33 and pi–alkyl interaction with Arg30 and Val148.

Additionally, the carbonyl functionality of benzoate stabilized the complex by making a hydrogen bond with Thr145. One of the 3-amino functional groups provided stability to the complex by forming a hydrogen bond with Val143. A similar type of hydrogen bonding interaction was exhibited by xanthenyl oxygen with Thr144. The aromatic ring further demonstrated promising pi–alkyl interaction with Val26 and Val148.

Similarly, rhein, 3-aminodibenzofuran, 5-(hydroxymethyl)-2-(dimethoxymethyl)furan, and dihydrorhodamine showed good affinity towards *LasR*, indicating multi-target potential of these molecules. Multi-target drugs are promising as they can be useful in reducing the QS-mediated drug resistance problem. Interactions of rhein with *LasR* are depicted in Fig. 11A. Here, the 4-OH group of scaffolds stabilized the ligand–receptor complex by forming a hydrogen bond with Thr75, Thr115, and Ser129, whereas 10-carbonyl functionality represented the same interaction with Ser129. The carboxylate group imparted stability by hydrogen bonding with Trp60 and pi–anion interaction with Trp88. The 9-carbonyl functional group interacted with Arg61 by stable hydrogen bonding. The aromatic rings of the scaffold exhibited promising pi–pi interactions with Tyr56 and Tyr64, along with pi–alkyl interaction with Leu36, Ile52, Val76, and Ala127. The 3D docked orientation of scaffold 3-aminodibenzofuran is depicted in Fig. 11B. Stability to this complex was imparted by a hydrogen bond between the 3-amino group with Leu110 and oxygen of furan with Trp60. The aromatic rings of the scaffold comfortably presented pi–pi interactions with Tyr56, Tyr64, Trp88, Phe101, and pi–alkyl hydrophobic interaction with Leu36, Ala105, Leu110. Interactions of 5-(hydroxymethyl)-2-(dimethoxymethyl)furan with *LasR* are presented in Fig. 11C. An aromatic ring of the scaffold was observed, forming a very stable pi–anion interaction with Asp73. The –OH group of hydroxymethyl imparted stability to the complex by exhibiting hydrogen bond interaction with Asp73. The same type of hydrogen bonding was observed between one of the methoxymethyl oxygen with Ser129. Further, the aromatic ring was comfortably found in the hydrophobic pocket of Tyr56, Tyr64, and Phe101. Dihydrorhodamine also showed favorable interaction with *LasR* (Fig. 11D). Methyl benzoate ring imparted stability by pi–alkyl hydrophobic interactions with Leu40, Ala50, Val76, Cys79, Leu125, and Ala127. The xanthenyl aromatic rings exhibited stability by pi–pi interaction with Tyr64 and pi–anion interaction with Asp73, and pi–alkyl hydrophobic interactions with Leu36, Ile52, Ala70, and Val76. One of the amine functionalities of the scaffold presented stable hydrogen bonds with Tyr47 and Asp65 and contributed to the ligand–receptor complex.

Results of *in silico* studies revealed that the various components of F-1, including all four scaffolds (rhein, 3-aminodibenzofuran, 5-(hydroxymethyl)-2-(dimethoxymethyl)furan, and dihydrorhodamine), showed promising interactions with both the targets under study (*Las*I and *LasR*). These antagonistic blockers either compete for the binding site of natural ligand inducer proteins (*Las*I) or the natural ligand-binding site on the quorum-sensing receptor proteins (*Las*R). The present data is in agreement with the results reported by Kordbacheh *et al.*[80] In this study, rutin and myricetin-3-*O*-rutinoside showed the highest affinity towards the *Las*R receptor with docking scores of −11.503 and −11.253 kJ mol^{-1}, respectively.

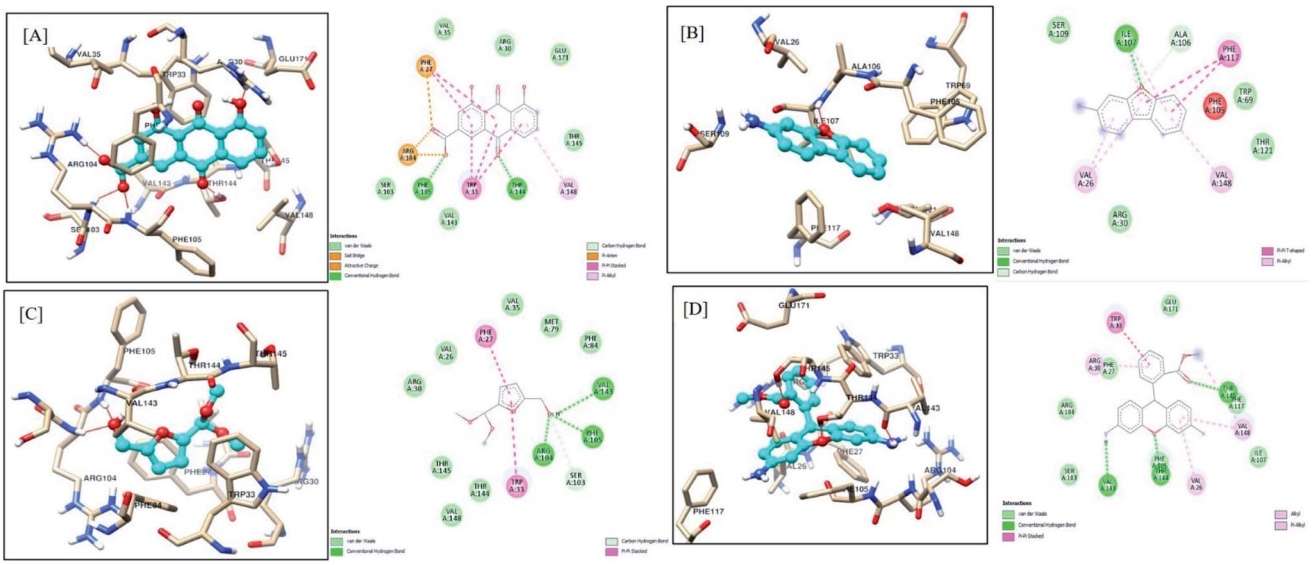

Fig. 11 Docking model of compounds identified by GCMS (A) rhein, (B) 3-aminodibenzofuran, (C) 5-(hydroxymethyl)-2-(dimethoxymethyl)furan and (D) dihydrorhodamine with LasR (PDB ID: 2UV0).

4. Conclusion

The study's overall results suggest that purified active secondary metabolites from *Cassia fistula* fruit pods and their active anthraquinone rhein substantially diminish the QS circuitry of *P. aeruginosa*. These natural phytoconstituents in various combinations with antimicrobial agents can be used to develop promising anti-virulence drug candidates based on their binding energies to impair bacterial pathogenicity by mitigating the QS mechanism.

Fundings

This research did not receive any grant from funding agencies in the public, commercial, or not-for-profit sectors.

Conflicts of interest

We have no conflicts of interest to declare.

Acknowledgements

This research sincerely acknowledges the Sophisticated Analytical Instrument Facility (SAIF), Indian Institute of Technology Bombay, Bombay, India for Scanning Microscopy facility, Department of Biosciences and Bioengineering (BSBE) for confocal microscopy analysis. We thank Dr Sandhya P. Koushika, Tata Institute of Fundamental Research, Mumbai, for providing *Caenorhabditis elegans* and *E. coli* OP50. We thank Dr Amisha Kamlesh Vora, Department of Pharmaceutical Chemistry, NMIMS, Mumbai, for providing LC-MS analysis of our samples. We also thank SVKM's NMIMS (Deemed University), Mumbai, India, for providing all the necessary facilities.

References

1 R. Laxminarayan and R. R. Chaudhury, Antibiotic Resistance in India : Drivers and Opportunities for Action, *PLoS Med.*, 2016, **3**, 1–7.
2 D. W. Macpherson, B. D. Gushulak, W. B. Baine, S. Bala, P. O. Gubbins, P. Holtom and M. Segarra-newnham, *Emerging Infect. Dis.*, 2009, **15**, 1727–1732.
3 F. F. Tuon, L. W. Gortz and J. L. Rocha, Risk Factors for Pan-Resistant Pseudomonas Aeruginosa Bacteremia and the Adequacy of Antibiotic Therapy, *Braz. J. Infect. Dis.*, 2012, **16**, 351–356.
4 X. Zhao, Z. Yu and T. Ding, Quorum-Sensing Regulation of Antimicrobial Resistance in Bacteria, *Microorganisms*, 2020, **8**, 1–21.
5 Z. Pang, R. Raudonis, B. R. Glick, T. J. Lin and Z. Cheng, Antibiotic Resistance in Pseudomonas Aeruginosa: Mechanisms and Alternative Therapeutic Strategies, *Biotechnol. Adv.*, 2019, **37**, 177–192.
6 T. B. Rasmussen and M. Givskov, A Bargain of Effects, *Microbiology*, 2006, **152**, 895–904.
7 T. H. Jakobsen, M. Van Gennip, R. K. Phipps, M. S. Shanmugham, L. D. Christensen, M. Alhede, M. E. Skindersoe, T. B. Rasmussen, K. Friedrich, F. Uthe, P. Ø. Jensen, C. Moser, K. F. Nielsen, L. Eberl, T. O. Larsen, D. Tanner, N. Høiby, T. Bjarnsholt and M. Givskov, Ajoene, a Sulfur-Rich Molecule from Garlic, Inhibits Genes Controlled by Quorum Sensing, *Antimicrob. Agents Chemother.*, 2012, **56**, 2314–2325.
8 J. P. Pearson, C. Van Delden and B. H. Iglewski, Active Efflux and Diffusion Are Involved in Transport of Pseudomonas Aeruginosa Cell-to-Cell Signals, *J. Bacteriol.*, 1999, **181**, 1203–1210.
9 J. P. Pearson, E. C. Pesci and B. H. Iglewski, Roles of Pseudomonas Aeruginosa Las and Rhl Quorum-Sensing

Systems in Control of Elastase and Rhamnolipid Biosynthesis Genes, *J. Bacteriol.*, 1997, **179**, 5756–5767.

10 Q. Jiang, J. Chen, C. Yang, Y. Yin, K. Yao and D. Song, Quorum Sensing: A Prospective Therapeutic Target for Bacterial Diseases, *BioMed Res. Int.*, 2019, DOI: **10.1155/2019/2015978**.

11 J. P. Pearson, L. Passador, B. H. Iglewski and E. P. Greenberg, A Second N-Acylhomoserine Lactone Signal Produced by Pseudomonas Aeruginosa, *Proc. Natl. Acad. Sci. U. S. A.*, 1995, **92**, 1490–1494.

12 S. Bhardwaj, S. Bhatia, S. Singh and F. Franco, Growing Emergence of Drug-Resistant Pseudomonas Aeruginosa and Attenuation of Its Virulence Using Quorum Sensing Inhibitors: A Critical Review, *Iran. J. Basic Med. Sci.*, 2021, **24**, 699–719.

13 M. Manefield, R. De Nys, N. Kumar, R. Read, M. Givskov, P. Steinberg and S. Kjelleberg, Evidence That Halogenated Furanones from Delisea Pulchra Inhibit Acylated Homoserine Lactone (AHL)-Mediated Gene Expression by Displacing the AHL Signal from Its Receptor Protein, *Microbiology*, 1999, **145**, 283–291.

14 M. Yang, F. Meng, W. Gu, F. Li, Y. Tao, Z. Zhang, F. Zhang, X. Yang, J. Li and J. Yu, Effects of Natural Products on Bacterial Communication and Network-Quorum Sensing, *BioMed Res. Int.*, 2020, DOI: **10.1155/2020/8638103**.

15 S. Haque, F. Ahmad, S. A. Dar, A. Jawed, R. K. Mandal, M. Wahid, M. Lohani, S. Khan, V. Singh and N. Akhter, Developments in Strategies for Quorum Sensing Virulence Factor Inhibition to Combat Bacterial Drug Resistance, *Microb. Pathog.*, 2018, **121**, 293–302.

16 B. Pejin, A. Ciric, J. Glamoclija, M. Nikolic and M. Sokovic, In Vitro Anti-Quorum Sensing Activity of Phytol, *Nat. Prod. Res.*, 2015, **29**, 374–377.

17 S. Hnamte, P. Parasuraman, S. Ranganathan, D. R. Ampasala, D. Reddy, R. N. Kumavath, K. Suchiang, S. K. Mohanty and S. Busi, Mosloflavone Attenuates the Quorum Sensing Controlled Virulence Phenotypes and Biofilm Formation in Pseudomonas Aeruginosa PAO1: In Vitro, In Vivo and In Silico Approach, *Microb. Pathog.*, 2019, **131**, 128–134.

18 J. Lee, Y. Kim, H. Seob, S. Yong, M. Hwan and J. Lee, Coumarins Reduce Biofilm Formation and the Virulence of Escherichia Coli O157:H7, *Phytomedicine*, 2014, **21**, 6–11.

19 K. Wang, B. Li and Y. Chen, Baicalein Attenuates the Quorum Sensing-Controlled Virulence Factors of Pseudomonas Aeruginosa and Relieves the Inflammatory Response in P. Aeruginosa - Infected Macrophages by Downregulating the MAPK and NF κ B Signal-Transduction Pathways, *Drug Des., Dev. Ther.*, 2016, **10**, 183–203.

20 I. A. S. V. Packiavathy, S. Priya, S. K. Pandian and A. V. Ravi, Inhibition of Biofilm Development of Uropathogens by Curcumin - An Anti-Quorum Sensing Agent from Curcuma Longa, *Food Chem.*, 2014, **148**, 453–460.

21 Y. T. Li, J. R. Huang, L. J. Li and L. S. Liu, Synergistic Activity of Berberine with Azithromycin against Pseudomonas Aeruginosa Isolated from Patients with Cystic Fibrosis of Lung In Vitro and In Vivo, *Cell. Physiol. Biochem.*, 2017, **42**, 1657–1669.

22 S. Zhou, A. Zhang and W. Chu, Phillyrin Is an Effective Inhibitor of Quorum Sensing with Potential as an Anti-Pseudomonas Aeruginosa Infection Therapy, *J. Vet. Med. Sci.*, 2019, **81**, 473–479.

23 D. N. Naik, S. Wahidullah and R. M. Meena, Attenuation of Pseudomonas Aeruginosa Virulence by Marine Invertebrate – Derived Streptomyces Sp, *Lett. Appl. Microbiol.*, 2012, **2**, 197–207.

24 F. M. Husain, I. Ahmad, M. Asif and Q. Tahseen, Influence of Clove Oil on Certain Quorum-Sensing-Regulated Functions and Biofilm of Pseudomonas Aeruginosa and Aeromonas Hydrophila, *J. Biosci.*, 2013, **38**, 835–844.

25 L. Kumar, S. Chhibber, R. Kumar, M. Kumar and K. Harjai, Zingerone Silences Quorum Sensing and Attenuates Virulence of Pseudomonas aeruginosa, *Fitoterapia*, 2015, **102**, 84–95.

26 M. Hentzer, K. Riedel, T. B. Rasmussen, A. Heydorn, J. B. Andersen, M. R. Parsek, S. A. Rice, L. Eberl, S. Molin, N. Høiby, S. Kjelleberg and M. Givskov, Inhibition of Quorum Sensing in Pseudomonas Aeruginosa Biofilm Bacteria by a Halogenated Furanone Compound, *Microbiology*, 2002, **148**, 87–102.

27 J. Ouyang, F. Sun, W. Feng, Y. Sun, X. Qiu, L. Xiong, Y. Liu and Y. Chen, Quercetin Is an Effective Inhibitor of Quorum Sensing, Biofilm Formation and Virulence Factors in Pseudomonas Aeruginosa, *J. Appl. Microbiol.*, 2016, **120**, 966–974.

28 D. K. Joung, H. Joung, D. W. Yang, D. Y. Kwon, J. G. Choi, S. Woo, D. Y. Shin, O. H. Kweon, K. T. Kweon and D. W. Shin, Synergistic Effect of Rhein in Combination with Ampicillin or Oxacillin against Methicillin-Resistant Staphylococcus Aureus, *Exp. Ther. Med.*, 2012, **3**, 608–612.

29 J. Azelmat, J. F. Larente and D. Grenier, The Anthraquinone Rhein Exhibits Synergistic Antibacterial Activity in Association with Metronidazole or Natural Compounds and Attenuates Virulence Gene Expression in Porphyromonas Gingivalis, *Arch. Oral Biol.*, 2015, **60**, 342–346.

30 X. Ding, B. Yin, L. Qian, Z. Zeng, Z. Yang, H. Li, Y. Lu and S. Zhou, Screening for Novel Quorum-Sensing Inhibitors to Interfere with the Formation of Pseudomonas aeruginosa Biofilm, *J. Med. Microbiol.*, 2011, **60**, 1827–1834.

31 R. M. Uckoo, G. K. Jayaprakasha and B. S. Patil, Rapid separation method of polymethoxyflavones from citrus using flash chromatography, *Sep. Purif. Technol.*, 2011, **81**, 151–158.

32 K. H. Mcclean, M. K. Winson, L. Fish, A. Taylor, S. R. Chhabra, M. Camara, M. Daykin, H. John, S. Swift, B. W. Bycroft, G. S. a B. Stewart and P. Williams, Quorum Sensing and Chrornobacteriurn Violaceurn : Exploitation of Violacein Production and Inhibition for the Detection of N-Acyl Homoserine Lactones, *Microbiology*, 1997, **143**, 3703–3711.

33 J. Luo, J. L. Kong, B. Y. Dong, H. Huang, K. Wang, L. H. Wu, C. C. Hou, Y. Liang, B. Li and Y. Q. Chen, Baicalein

Attenuates the Quorum Sensing-Controlled Virulence Factors of Pseudomonas Aeruginosa and Relieves the Inflammatory Response in p. Aeruginosa-Infected Macrophages by Downregulating the MAPK and NFκB Signal-Transduction Pathways, *Drug Des., Dev. Ther.*, 2016, **10**, 183–203.

34 A. Kulkarni, M. Govindappa, C. P. Chandrappa, Y. L. Ramachandra and P. S. Koka, Phytochemical Analysis of Cassia Fistula and Its In Vitro Antimicrobial, Antioxidant Activities, *Adv. Med. Plant. Res.*, 2015, **3**, 8–17.

35 S. L. Jothy, Z. Zakaria, Y. Chen, Y. L. Lau, L. Y. Latha, L. N. Shin and S. Sasidharan, Bioassay-Directed Isolation of Active Compounds with Antiyeast Activity from a Cassia Fistula Seed Extract, *Molecules*, 2011, **16**, 7583–7592.

36 S. V. P. Issac Abraham, A. Palani, B. R. Ramaswamy, K. P. Shunmugiah and V. R. Arumugam, Antiquorum Sensing and Antibiofilm Potential of Capparis Spinosa, *Arch. Med. Res.*, 2011, **42**, 658–668.

37 V. C. Gala, N. R. John, A. M. Bhagwat, A. G. Datar, P. S. Kharkar and K. B. Desai, Attenuation of Quorum Sensing-Regulated Behaviour by Tinospora Cordifolia Extract & Identification of Its Active Constituents, *Indian J. Med. Res.*, 2016, 92–103.

38 I. A. S. V. Packiavathy, P. Agilandeswari, K. S. Musthafa, S. Karutha Pandian and A. V. Ravi, Antibiofilm and Quorum Sensing Inhibitory Potential of Cuminum Cyminum and Its Secondary Metabolite Methyl Eugenol against Gram Negative Bacterial Pathogens, *Food Res. Int.*, 2015, **1**, 8–17.

39 F. A. Qais, M. S. Khan and I. Ahmad, Broad-Spectrum Quorum Sensing and Biofilm Inhibition by Green Tea against Gram-Negative Pathogenic Bacteria: Deciphering the Role of Phytocompounds through Molecular Modelling, *Microb. Pathog.*, 2019, **126**, 379–392.

40 F. Pantanella, F. Berlutti, C. Passariello, S. Sarli, C. Morea and S. Schippa, Violacein and Biofilm Production in Janthinobacterium Lividum, *J. Appl. Microbiol.*, 2007, **102**, 992–999.

41 M. D. Shah, P. S. Kharkar, N. U. Sahu, Z. Peerzada and K. B. Desai, A Novel Hit Exhibiting Quorum-Sensing Inhibition in: Pseudomonas Aeruginosa via LasIR/RhlIR Circuitry, *RSC Adv.*, 2019, **9**, 40228–40239.

42 E. Kessler, M. Safrin, J. C. Olson and D. E. Ohman, Secreted LasA of Pseudomonas Aeruginosa Is a Staphylolytic Protease, *J. Biol. Chem.*, 1993, **268**, 7503–7508.

43 A. Moayedi, J. Nowroozi and A. Akhavan Sepahy, Effect of Fetal and Adult Bovine Serum on Development of Pyocyanin Production in Clinical and Soil Isolates of Pseudomonas Aeruginosa, *Iran. J. Basic Med. Sci.*, 2017, **20**, 1331–1338.

44 A. Adonizio, S. M. Leal, F. M. Ausubel and K. Mathee, Attenuation of Pseudomonas Aeruginosa Virulence by Medicinal Plants in a Caenorhabditis Elegans Model System, *J. Med. Microbiol.*, 2008, **57**, 809–813.

45 C. T. O'Loughlin, L. C. Miller, A. Siryaporn, K. Drescher, M. F. Semmelhack and B. L. Bassler, A Quorum-Sensing Inhibitor Blocks Pseudomonas Aeruginosa Virulence and Biofilm Formation, *Proc. Natl. Acad. Sci. U. S. A.*, 2013, **110**, 17981–17986.

46 X. Xu, W. Ho, X. Zhang, N. Bertrand and O. Farokhzad, Cancer Nanomedicine: From Targeted Delivery to Combination Therapy, *Trends Mol. Med.*, 2015, **21**, 223–232.

47 A. K. Koch, O. Kappeli, A. Fiechter and J. Reiser, Hydrocarbon assimilation and biosurfactant production in Pseudomonas aeruginosa mutants., *J. Bacteriol.*, 1991, **173**, 4212–4219.

48 I. Vallet, S. P. Diggle, R. E. Stacey, M. Cámara, I. Ventre, S. Lory, A. Lazdunski, P. Williams and A. Filloux, Biofilm Formation in Pseudomonas Aeruginosa: Fimbrial Cup Gene Clusters Are Controlled by the Transcriptional Regulator MvaT, *J. Bacteriol.*, 2004, **186**, 2880–2890.

49 P. N. Okusa, T. Rasamiravaka, O. Vandeputte, C. Stévigny, M. El Jaziri and P. Duez, Extracts of Cordia Gilletii de Wild (Boraginaceae) Quench the Quorum Sensing of Pseudomonas Aeruginosa, *J. Intercult. Ethnopharmacol.*, 2014, **3**, 138–143.

50 C. De La Fuente-Núñez, V. Korolik, M. Bains, U. Nguyen, E. B. Breidenstein, S. Horsman, S. Lewenza, L. Burrows and R. E. Hancock, Inhibition of bacterial biofilm formation and swarming motility by a small synthetic cationic peptide, *Antimicrob. Agents Chemother*, 2012, **56**, 2696–2704.

51 J. Zhang, X. Rui, L. Wang, Y. Guan, X. Sun and M. Dong, Polyphenolic Extract from Rosa Rugosa Tea Inhibits Bacterial Quorum Sensing and Biofilm Formation, *Food Control*, 2014, **42**, 125–131.

52 V. K. Singh, A. Mishra and B. Jha, Anti-Quorum Sensing and Anti-Biofilm Activity of Delftia Tsuruhatensis Extract by Attenuating the Quorum Sensing-Controlled Virulence Factor Production in Pseudomonas Aeruginosa, *Front. Cell. Infect. Microbiol.*, 2017, **7**, 1–16.

53 H. Li, X. Li, Z. Wang, Y. Fu, Q. Ai, Y. Dong and J. Yu, Autoinducer-2 Regulates Pseudomonas Aeruginosa PAO1 Biofilm Formation and Virulence Production in a Dose-Dependent Manner, *BMC Microbiol.*, 2015, **15**, 1–8.

54 S. Mahajan-Miklos, M. W. Tan, L. G. Rahme and F. M. Ausubel, Molecular Mechanisms of Bacterial Virulence Elucidated Using a Pseudomonas Aeruginosa-Caenorhabditis Elegans Pathogenesis Model, *Cell*, 1999, **96**, 47–56.

55 M. W. Tan, S. Mahajan-Miklos and F. M. Ausubel, Killing of Caenorhabditis Elegans by Pseudomonas Aeruginosa Used to Model Mammalian Bacterial Pathogenesis, *Proc. Natl. Acad. Sci. U. S. A.*, 1999, **96**, 715–720.

56 M. F. Sanner and L. Jolla, Python: a programming language for software integration and development, *J. Mol. Graphics Modell.*, 1999, **17**, 55–84.

57 G. M. Morris, H. Ruth, W. Lindstrom, M. F. Sanner, R. K. Belew, D. S. Goodsell and A. J. Olson, Automated Docking with Selective Receptor Flexibility, *J. Comput. Chem.*, 2009, **30**, 2785–2791.

58 T. A. Gould, H. P. Schweizer and M. E. A. Churchill, Structure of the Pseudomonas Aeruginosa Acyl- Homoserinelactone Synthase LasI, *Mol. Microbiol.*, 2004, **53**, 1135–1146.

59 E. F. Pettersen, T. D. Goddard, C. C. Huang, G. S. Couch, D. M. Greenblatt, E. C. Meng and T. E. Ferrin, UCSF Chimera — A Visualization System for Exploratory Research and Analysis, *J. Comput. Chem.*, 2004, **13**, 1605–1612.

60 R. J. C. Mclean, L. S. Pierson and C. Fuqua, A Simple Screening Protocol for the Identification of Quorum Signal Antagonists, *J. Microbiol. Methods*, 2004, **58**, 351–360.

61 F. M. Husain, I. Ahmad, A. S. Al-thubiani, H. H. Abulreesh, I. M. Alhazza and F. Aqil, Leaf Extracts of Mangifera Indica L. Inhibit Quorum Sensing – Regulated Production of Virulence Factors and Biofilm in Test Bacteria, *Front. Microbiol.*, 2017, **8**, 1–12.

62 A. Kulkarni, M. Govindappa, Y. L. Ramachandra and K. Prasad, GC-MS analysis of methanol extract of Cassia fistula and its in vitro anticancer activity on human prostate cancer cell line, *Indo Am. J. Pharm. Res.*, 2015, **5**, 937–944.

63 H. S. Vasavi, A. B. Arun and P. D. Rekha, Anti-Quorum Sensing Activity of Psidium Guajava L. Flavonoids against Chromobacterium Violaceum and Pseudomonas Aeruginosa PAO1, *Microbiol. Immunol.*, 2014, **58**, 286–293.

64 W. Wang, M. I. Arshad, M. Khurshid, M. H. Rasool, M. A. Nisar, M. A. Aslam and M. U. Qamar, Antibiotic Resistance : A Rundown of a Global Crisis, *Infect. Drug Resist.*, 2018, **11**, 1645–1658.

65 M. Kalia, V. K. Yadav, P. K. Singh, D. Sharma, S. S. Narvi and V. Agarwal, Exploring the Impact of Parthenolide as Anti-Quorum Sensing and Anti-Biofilm Agent against Pseudomonas Aeruginosa, *Life Sci.*, 2018, **199**, 96–103.

66 J. B. Aswathanarayan and R. R Vittal, Inhibition of Biofilm Formation and Quorum Sensing Mediated Phenotypes by Berberine in: Pseudomonas Aeruginosa and Salmonella Typhimurium, *RSC Adv.*, 2018, **8**, 36133–36141.

67 L. Zhou, H. Zheng, Y. Tang, W. Yu and Q. Gong, Eugenol Inhibits Quorum Sensing at Sub-Inhibitory Concentrations, *Biotechnol. Lett.*, 2013, **4**, 1–7.

68 A. Adonizio, K. F. Kong and K. Mathee, Inhibition of Quorum Sensing-Controlled Virulence Factor Production in Pseudomonas Aeruginosa by South Florida Plant Extracts, *Antimicrob. Agents Chemother.*, 2008, **52**, 198–203.

69 C. Winstanley and J. L. Fothergill, The Role of Quorum Sensing in Chronic Cystic Fibrosis Pseudomonas Aeruginosa Infections, *FEMS Microbiol. Lett.*, 2009, **290**, 1–9.

70 K. Brindhadevi, F. Lewis-Oscar, E. Mylonakis, S. Shanmugam, T. N. Verma and A. Pugazhendhi, Biofilm and Quorum Sensing Mediated Pathogenicity in Pseudomonas Aeruginosa, *Process Biochem.*, 2020, **96**, 49–57.

71 T. R. D. E. Kievit, R. Gillis, S. Marx and C. Brown, Quorum-Sensing Genes in Pseudomonas Aeruginosa Biofilms : Their Role and Expression Patterns, *Appl. Environ. Microbiol.*, 2001, **67**, 1865–1873.

72 J. W. Zhou, H. Z. Luo, H. Jiang, T. K. Jian, Z. Q. Chen and A. Q. Jia, Hordenine: A Novel Quorum Sensing Inhibitor and Antibiofilm Agent against Pseudomonas Aeruginosa, *J. Agric. Food Chem.*, 2018, **66**, 1620–1628.

73 I. Aleksic, J. Jeremic, D. Milivojevic, T. Ilic-Tomic, S. Šegan, M. Zlatović, D. M. Opsenica and L. Senerovic, N-Benzyl Derivatives of Long-Chained 4-Amino-7-Chloro-Quionolines as Inhibitors of Pyocyanin Production in Pseudomonas Aeruginosa, *ACS Chem. Biol.*, 2019, **14**, 2800–2809.

74 M. T. T. Thi, D. Wibowo and B. H. A. Rehm, Pseudomonas Aeruginosa Biofilms, *Int. J. Mol. Sci.*, 2020, **21**, 1–25.

75 J. Rajkumari, S. Borkotoky, A. Murali, K. Suchiang, S. K. Mohanty and S. Busi, Cinnamic Acid Attenuates Quorum Sensing Associated Virulence Factors and Biofilm Formation in Pseudomonas Aeruginosa PAO1, *Biotechnol. Lett.*, 2018, **40**, 1087–1100.

76 V. Venturi, Regulation of Quorum Sensing in Pseudomonas, *FEMS Microbiol. Rev.*, 2006, **30**, 274–291.

77 M. N. Taha, A. E. Saafan, A. Ahmedy, E. El Gebaly and A. S. Khairalla, Two Novel Synthetic Peptides Inhibit Quorum Sensing-Dependent Biofilm Formation and Some Virulence Factors in Pseudomonas Aeruginosa PAO1, *J. Microbiol.*, 2019, **57**, 618–625.

78 T. B. Rasmussen and M. Givskov, Quorum Sensing Inhibitors: A Bargain of Effects, *Microbiology*, 2006, **152**, 895–904.

79 P. Sankar Ganesh and V. Ravishankar Rai, Attenuation of Quorum-Sensing-Dependent Virulence Factors and Biofilm Formation by Medicinal Plants against Antibiotic Resistant Pseudomonas Aeruginosa, *J. Tradit. Complement. Med.*, 2018, **8**, 170–177.

80 H. Kordbacheh, F. Eftekhar and S. N. Ebrahimi, Microbial Pathogenesis Anti-Quorum Sensing Activity of Pistacia Atlantica against Pseudomonas Aeruginosa PAO1 and Identification of Its Bioactive Compounds, *Microb. Pathog.*, 2017, **110**, 390–398.